67 ADDITIONAL L DWARFS DISCOVERED BY THE TWO MICRON ALL SKY SURVEY[1]

J. DAVY KIRKPATRICK,[2] I. NEILL REID,[3] JAMES LIEBERT,[4] JOHN E. GIZIS,[2] ADAM J. BURGASSER,[5] DAVID G. MONET,[6]
CONARD C. DAHN,[6] BRANT NELSON,[2] AND RIK J. WILLIAMS[7]

ABSTRACT

We present JHK_s photometry, far red spectra, and spectral classifications for an additional 67 L dwarfs discovered by the Two Micron All Sky Survey. One of the goals of this new search was to locate more examples of the latest L dwarfs. Of the 67 new discoveries, 17 have types of L6 or later. Analysis of these new discoveries shows that Hα emission has yet to be convincingly detected in any L dwarf later than type L4.5, indicating a decline or absence of chromospheric activity in the latest L dwarfs. Further analysis shows that 16 (and possibly four more) of the new L dwarfs are lithium brown dwarfs and that the average line strength for those L dwarfs showing lithium increases until type ∼L6.5 V, then declines for later types. This disappearance may be the first sign of depletion of atomic lithium as it begins to form into lithium-bearing molecules. Another goal of the search was to locate nearer, brighter L dwarfs of all subtypes. Using absolute magnitudes for 17 L dwarf systems with trigonometric parallax measurements, we develop spectrophotometric relations to estimate distances to the other L dwarfs. Of the 67 new discoveries, 21 have photometric distances placing them within 25 pc of the Sun. A table of all known L and T dwarfs believed to lie within 25 pc—53 in total — is also presented. Using the distance measurement of the coolest L dwarf known, we calculate that the gap in temperature between L8 and the warmest known T dwarfs is less than 350 K and probably much less. If the transition region between the two classes spans a very small temperature interval, this would explain why no transition objects have yet been uncovered. This evidence, combined with model fits to low-resolution spectra of late M and early L dwarfs, indicates that L-class objects span the range $1300 \text{ K} \lesssim T_{\rm eff} \lesssim 2000 \text{ K}$. The near-infrared color-color diagram shows that L dwarfs fall along a natural, redder extension of the well-known M dwarf track. These near-infrared colors get progressively redder for later spectral types, with the L dwarf sequence abruptly ending near $(J-H, H-K_s, J-K_s) \approx (1.3, 0.8, 2.1)$.

Key words: infrared radiation — stars: atmospheres — stars: distances —
stars: fundamental parameters — stars: low-mass, brown dwarfs

1. INTRODUCTION

In 1993, the first spectrum of what would later be known as an L dwarf was published (Kirkpatrick, Henry, & Liebert 1993). This object, GD 165B, had been discovered earlier by Becklin & Zuckerman (1988) as a resolved companion to a nearby white dwarf. For several years, GD 165B remained in a class by itself. Then, beginning in 1997, an explosion of discoveries proved that L dwarfs are quite common in the solar neighborhood (Reid et al. 1999; see also Delfosse et al. 1997; Ruiz, Leggett, & Allard 1997; Rebolo et al. 1998; Kirkpatrick et al. 1999, hereafter Paper I; Goldman et al. 1999; Martín et al. 1999b; Fan et al. 2000).

Providing a historical parallel to the L dwarfs are the T dwarfs, even cooler objects spectroscopically defined as those showing methane at K band (Paper I). In 1995, the first spectrum of a T dwarf was published (Oppenheimer et al. 1995). This object, Gl 229B, had been discovered as a companion to a nearby M dwarf by Nakajima et al. (1995) and remained in a class by itself for several years. Then beginning in 1999, an explosion of discoveries proved that observable T dwarfs have a space density comparable to that of L dwarfs (Strauss et al. 1999; Burgasser et al. 1999, 2000a, 2000c; Cuby et al. 1999; Tsvetanov et al. 2000).

Despite the implied space density and the subsequent profusion of cooler, T dwarf discoveries, the number of known L dwarfs is still small. Additional examples, including a larger number of late L dwarfs and nearer (brighter) examples of all L subtypes, are needed for further studies, including parallax measurement, luminosity and temperature determination, kinematics, binarity, and detailed spectroscopic analyses related to magnetic activity, lithium frequency, atmospheric abundances, dust formation, etc. To this end, we present here another 67 L dwarfs found during follow-up of candidates selected from the Two Micron All Sky Survey (2MASS) data.

[1] Portions of the data presented herein were obtained at the W. M. Keck Observatory, which is operated as a scientific partnership among the California Institute of Technology, the University of California, and the National Aeronautics and Space Administration. The observatory was made possible by the generous financial support of the W. M. Keck Foundation.

[2] Infrared Processing and Analysis Center, Mail Stop 100-22, California Institute of Technology, Pasadena, CA 91125; davy@ipac.caltech.edu, gizis@ipac.caltech.edu, nelson@ipac.caltech.edu.

[3] Department of Physics and Astronomy, University of Pennsylvania, 209 South 33d Street, Philadelphia, PA 19104-6396; inr@herschel.physics.upenn.edu.

[4] Steward Observatory, University of Arizona, 933 North Cherry Avenue, Tucson, AZ 85721-0065; liebert@as.arizona.edu.

[5] Department of Physics, Mail Stop 103-33, California Institute of Technology, Pasadena, CA 91125; diver@its.caltech.edu.

[6] US Naval Observatory, Flagstaff Station, P.O. Box 1149, Flagstaff, AZ 86002; dgm@nofs.navy.mil, dahn@nofs.navy.mil.

[7] Department of Astronomy, MSC 152, California Institute of Technology, Pasadena, CA 91126-0152.

TABLE 1

DATA FOR NEW L DWARFS

L Dwarf[a] (1)	J (2)	H (3)	K_s (4)	$J-K_s$ (5)	$J-H$ (6)	$H-K_s$ (7)	Telescope[b] (8)	Date (UT) (9)	Exposure (s) (10)
2MASSW J0015447+351603...	13.82 ± 0.04	12.81 ± 0.03	12.24 ± 0.03	1.58 ± 0.05	1.00 ± 0.05	0.57 ± 0.05	K	1999 Jul 17	1200
2MASSI J0028394+150141	16.49 ± 0.14	15.33 ± 0.10	14.62 ± 0.13	1.87 ± 0.19	1.16 ± 0.17	0.71 ± 0.16	K	1998 Dec 14	3600
								1998 Dec 16	2400
2MASSW J0030300−145033...	16.79 ± 0.16	15.36 ± 0.09	14.38 ± 0.08	2.41 ± 0.18	1.44 ± 0.18	0.98 ± 0.12	K	1999 Jul 18	2400
2MASSW J0036159+182110...	12.44 ± 0.04	11.58 ± 0.03	11.03 ± 0.03	1.41 ± 0.05	0.86 ± 0.05	0.55 ± 0.04	K	1998 Dec 14	1800
								1998 Dec 16	900
2MASSW J0051107−154417...	15.23 ± 0.05	14.15 ± 0.04	13.42 ± 0.05	1.81 ± 0.07	1.08 ± 0.07	0.72 ± 0.06	K	1999 Jul 18	1200
2MASSW J0058425−065123...	14.32 ± 0.03	13.45 ± 0.03	12.91 ± 0.04	1.41 ± 0.05	0.88 ± 0.04	0.54 ± 0.04	K	1999 Jul 17	900
2MASSI J0103320+193536	16.26 ± 0.09	14.88 ± 0.06	14.15 ± 0.07	2.11 ± 0.11	1.38 ± 0.11	0.73 ± 0.09	K	1998 Dec 14	2400
								1998 Dec 16	2400
2MASSW J0135358+120522...	14.43 ± 0.04	13.44 ± 0.03	12.86 ± 0.03	1.57 ± 0.05	0.99 ± 0.05	0.57 ± 0.05	K	1999 Jul 17	900
2MASSW J0205034+125142...	15.69 ± 0.06	14.47 ± 0.05	13.68 ± 0.05	2.01 ± 0.08	1.22 ± 0.08	0.79 ± 0.07	K	1998 Dec 14	2400
2MASSW J0208183+254253...	14.02 ± 0.03	13.11 ± 0.04	12.58 ± 0.04	1.44 ± 0.05	0.91 ± 0.05	0.53 ± 0.05	K	1999 Jul 17	600
2MASSW J0208236+273740...	15.70 ± 0.07	14.55 ± 0.06	13.87 ± 0.06	1.83 ± 0.09	1.15 ± 0.09	0.68 ± 0.08	K	1998 Dec 15	2400
2MASSW J0208549+250048...	16.24 ± 0.10	15.00 ± 0.09	14.38 ± 0.08	1.86 ± 0.13	1.24 ± 0.13	0.62 ± 0.12	K	1998 Dec 15	2400
2MASSI J0224367+253704	16.55 ± 0.11	15.42 ± 0.09	14.67 ± 0.09	1.88 ± 0.14	1.13 ± 0.14	0.75 ± 0.13	K	1998 Dec 15	2400
								1998 Dec 16	2400
2MASSI J0302012+135814	16.55 ± 0.12	15.46 ± 0.09	14.55 ± 0.09	2.00 ± 0.15	1.09 ± 0.15	0.91 ± 0.13	K	1998 Dec 14	2400
								1998 Dec 16	1200
2MASSW J0306268+154514...	17.12 ± 0.19	16.24 ± 0.22	15.16 ± 0.14	1.96 ± 0.24	0.88 ± 0.29	1.08 ± 0.26	K	1998 Dec 24	3600
2MASSW J0309088−194938...	15.82 ± 0.06	14.67 ± 0.06	14.08 ± 0.07	1.74 ± 0.09	1.16 ± 0.09	0.59 ± 0.09	K	1999 Jul 18	1200
2MASSW J0310599+164816...	16.43 ± 0.11	14.95 ± 0.07	14.40 ± 0.10	2.03 ± 0.15	1.48 ± 0.13	0.55 ± 0.12	K	1998 Dec 15	4800
								1998 Dec 16	3600
2MASSI J0328426+230205	16.67 ± 0.14	15.62 ± 0.13	14.84 ± 0.13	1.83 ± 0.19	1.05 ± 0.19	0.78 ± 0.18	K	1998 Dec 15	3600
								1998 Dec 16	3600
								1999 Mar 04	2400
2MASSW J0337036−175807...	15.60 ± 0.06	14.39 ± 0.05	13.57 ± 0.04	2.03 ± 0.07	1.21 ± 0.07	0.83 ± 0.06	K	1999 Jul 17	2400
2MASSI J0409095+210439	15.55 ± 0.07	14.46 ± 0.06	13.84 ± 0.06	1.71 ± 0.09	1.09 ± 0.09	0.62 ± 0.08	K	1998 Dec 16	1200
2MASSW J0708213+295035...	16.75 ± 0.12	15.54 ± 0.12	14.69 ± 0.09	2.06 ± 0.15	1.21 ± 0.17	0.85 ± 0.15	K	1998 Dec 24	2400
2MASSW J0740096+321203...	16.17 ± 0.09	14.84 ± 0.06	14.18 ± 0.06	1.99 ± 0.11	1.33 ± 0.11	0.66 ± 0.08	K	1998 Dec 14	2400
2MASSI J0746425+200032	11.74 ± 0.03	11.00 ± 0.04	10.49 ± 0.03	1.25 ± 0.04	0.74 ± 0.05	0.51 ± 0.05	K	1998 Dec 24	600
2MASSI J0753321+291711	15.49 ± 0.05	14.49 ± 0.05	13.85 ± 0.06	1.64 ± 0.08	1.00 ± 0.07	0.64 ± 0.08	K	1998 Dec 24	2400
2MASSI J0756252+124456	16.66 ± 0.14	15.76 ± 0.15	14.67 ± 0.12	1.99 ± 0.18	0.90 ± 0.21	1.09 ± 0.19	K	1998 Dec 15	2400
								1998 Dec 16	1200
2MASSW J0801405+462850...	16.29 ± 0.14	15.44 ± 0.15	14.54 ± 0.11	1.75 ± 0.18	0.85 ± 0.21	0.90 ± 0.19	K	1998 Dec 15	2400
2MASSW J0820299+450031...	16.29 ± 0.11	15.00 ± 0.09	14.23 ± 0.08	2.06 ± 0.14	1.29 ± 0.14	0.77 ± 0.12	K	1998 Dec 14	3600
								1998 Dec 16	2400
2MASSI J0825196+211552	15.12 ± 0.04	13.79 ± 0.04	13.05 ± 0.04	2.07 ± 0.06	1.33 ± 0.06	0.74 ± 0.06	K	1998 Dec 14	2400
2MASSW J0829066+145622...	14.72 ± 0.03	13.79 ± 0.04	13.12 ± 0.05	1.60 ± 0.06	0.93 ± 0.05	0.67 ± 0.06	K	1998 Dec 15	1200
2MASSW J0829570+265510...	17.08 ± 0.20	15.74 ± 0.14	14.81 ± 0.10	2.27 ± 0.30	1.34 ± 0.24	0.93 ± 0.17	K	1998 Dec 24	2400
2MASSW J0832045−012835...	14.13 ± 0.03	13.31 ± 0.03	12.69 ± 0.03	1.44 ± 0.04	0.82 ± 0.04	0.62 ± 0.04	K	1999 Mar 04	1200
2MASSW J0920122+351742...	15.59 ± 0.07	14.66 ± 0.07	13.93 ± 0.08	1.66 ± 0.11	0.93 ± 0.10	0.73 ± 0.11	K	1998 Dec 24	2400
2MASSW J0928397−160312...	15.34 ± 0.05	14.30 ± 0.04	13.64 ± 0.05	1.70 ± 0.07	1.04 ± 0.06	0.66 ± 0.06	K	1998 Dec 25	2400
2MASSW J0929336+342952...	16.60 ± 0.13	15.52 ± 0.12	14.62 ± 0.11	1.98 ± 0.17	1.08 ± 0.18	0.90 ± 0.16	K	1998 Dec 15	2400
								1998 Dec 16	3600
2MASSW J0944027+313132...	15.50 ± 0.06	14.61 ± 0.06	13.98 ± 0.05	1.52 ± 0.08	0.89 ± 0.08	0.63 ± 0.08	K	1998 Dec 25	2400
2MASSW J0951054+355801...	17.29 ± 0.25	15.77 ± 0.14	15.04 ± 0.12	2.25 ± 0.28	1.52 ± 0.29	0.73 ± 0.18	K	1998 Dec 15	3600
								1998 Dec 16	3600
2MASSI J1029216+162652	14.31 ± 0.04	13.35 ± 0.04	12.61 ± 0.04	1.70 ± 0.06	0.96 ± 0.06	0.74 ± 0.06	K	1998 Dec 14	1200
2MASSW J1035245+250745...	14.70 ± 0.04	13.88 ± 0.04	13.28 ± 0.04	1.42 ± 0.06	0.82 ± 0.06	0.60 ± 0.06	K	1998 Dec 25	1200
2MASSW J1102337−235945...	17.04 ± 0.19	15.61 ± 0.13	14.79 ± 0.09	2.25 ± 0.21	1.43 ± 0.23	0.82 ± 0.16	K	1998 Dec 14	2400
								1998 Dec 16	2400
2MASSW J1112257+354813...	14.57 ± 0.04	13.47 ± 0.04	12.69 ± 0.05	1.88 ± 0.06	1.10 ± 0.06	0.78 ± 0.06	K	1998 Dec 14	1200
								1999 Mar 04	1200
								1999 Mar 05	3600
2MASSW J1123556+412228...	16.07 ± 0.08	15.14 ± 0.08	14.34 ± 0.06	1.73 ± 0.10	0.93 ± 0.11	0.80 ± 0.10	K	1998 Dec 25	2400
2MASSW J1239272+551537...	14.67 ± 0.03	13.54 ± 0.04	12.74 ± 0.03	1.93 ± 0.05	1.13 ± 0.05	0.80 ± 0.05	K	1999 Jul 17	1200
2MASSW J1246467+402715...	15.00 ± 0.04	13.98 ± 0.04	13.30 ± 0.04	1.70 ± 0.06	1.02 ± 0.06	0.68 ± 0.06	K	1998 Dec 24	600
2MASSI J1332286+263508	16.11 ± 0.10	15.10 ± 0.09	14.36 ± 0.08	1.75 ± 0.13	1.01 ± 0.13	0.74 ± 0.12	K	1998 Dec 25	1200
2MASSW J1338261+414034...	14.22 ± 0.03	13.30 ± 0.03	12.75 ± 0.04	1.47 ± 0.05	0.92 ± 0.04	0.55 ± 0.05	K	1998 Dec 14	1200
2MASSW J1343167+394508...	16.18 ± 0.08	14.85 ± 0.06	14.11 ± 0.06	2.07 ± 0.10	1.33 ± 0.10	0.74 ± 0.08	K	1998 Dec 14	1200
2MASSW J1411175+393636...	14.68 ± 0.04	13.81 ± 0.07	13.27 ± 0.05	1.41 ± 0.06	0.87 ± 0.08	0.54 ± 0.09	K	1999 Mar 05	1800
2MASSW J1412244+163312...	13.89 ± 0.04	13.06 ± 0.03	12.59 ± 0.03	1.30 ± 0.05	0.83 ± 0.05	0.47 ± 0.04	K	1998 Dec 25	1200
2MASSW J1438549−130910...	15.53 ± 0.05	14.52 ± 0.05	13.88 ± 0.06	1.65 ± 0.08	1.01 ± 0.07	0.64 ± 0.08	K	1999 Mar 04	2400

TABLE 1—*Continued*

L Dwarf[a] (1)	J (2)	H (3)	K_s (4)	$J - K_s$ (5)	$J - H$ (6)	$H - K_s$ (7)	Telescope[b] (8)	Date (UT) (9)	Exposure (s) (10)
2MASSW J1449378+235537...	15.80 ± 0.08	15.07 ± 0.09	14.34 ± 0.10	1.46 ± 0.13	0.73 ± 0.12	0.73 ± 0.13	P	1998 Jul 19	1200
2MASSW J1507476−162738...	12.82 ± 0.03	11.90 ± 0.03	11.30 ± 0.03	1.52 ± 0.04	0.92 ± 0.04	0.60 ± 0.04	K	1998 Dec 24	900
								1999 Mar 05	1800
2MASSW J1523226+301456...	16.32 ± 0.11	15.00 ± 0.07	14.24 ± 0.07	2.09 ± 0.13	1.33 ± 0.13	0.76 ± 0.10	K	1998 Dec 24	3600
								1998 Dec 25	4600
								1999 Mar 04	3600
								1999 Mar 31	4800
2MASSI J1526140+204341	15.62 ± 0.07	14.50 ± 0.06	13.92 ± 0.06	1.70 ± 0.09	1.12 ± 0.09	0.58 ± 0.08	P	1998 Sep 20	1200
2MASSI J1600054+170832	16.10 ± 0.10	15.13 ± 0.08	14.67 ± 0.12	1.43 ± 0.16	0.97 ± 0.13	0.46 ± 0.14	K	1999 Jul 16	1200
2MASSW J1615441+355900...	14.55 ± 0.04	13.55 ± 0.04	12.89 ± 0.05	1.67 ± 0.06	1.00 ± 0.06	0.66 ± 0.06	K	1999 Jul 16	1200
2MASSI J1656188+283506	17.10 ± 0.20	15.93 ± 0.15	14.96 ± 0.16	2.14 ± 0.26	1.17 ± 0.25	0.97 ± 0.22	K	1998 Aug 13	2400
								1999 Jul 17	1200
2MASSI J1711457+223204	17.10 ± 0.19	15.77 ± 0.11	14.69 ± 0.10	2.41 ± 0.21	1.33 ± 0.22	1.08 ± 0.15	K	1998 Aug 13	2400
2MASSI J1726000+153819	15.65 ± 0.07	14.46 ± 0.06	13.64 ± 0.05	2.01 ± 0.09	1.19 ± 0.09	0.82 ± 0.08	K	1998 Aug 13	2400
2MASSW J1728114+394859...	15.96 ± 0.08	14.78 ± 0.07	13.90 ± 0.05	2.07 ± 0.10	1.18 ± 0.11	0.88 ± 0.09	K	1999 Jul 16	2400
2MASSW J1743415+212707...	15.80 ± 0.09	14.78 ± 0.07	14.29 ± 0.10	1.51 ± 0.13	1.02 ± 0.11	0.49 ± 0.12	K	1999 Jul 17	1200
2MASSW J1841086+311727...	16.12 ± 0.10	14.97 ± 0.07	14.18 ± 0.08	1.95 ± 0.13	1.15 ± 0.12	0.80 ± 0.11	K	1999 Jul 18	2400
2MASSI J2054358+151904	16.51 ± 0.13	15.58 ± 0.14	14.82 ± 0.16	1.69 ± 0.21	0.93 ± 0.19	0.76 ± 0.21	K	1998 Aug 13	2400
2MASSI J2057153+171515	16.11 ± 0.11	15.21 ± 0.09	14.57 ± 0.13	1.54 ± 0.17	0.90 ± 0.14	0.64 ± 0.16	K	1999 Jul 17	1200
2MASSW J2101154+175658...	16.87 ± 0.19	15.70 ± 0.14	15.04 ± 0.19	1.83 ± 0.27	1.17 ± 0.24	0.66 ± 0.24	K	1998 Aug 13	3600
2MASSW J2206540−421721...	15.57 ± 0.07	14.48 ± 0.06	13.60 ± 0.06	1.97 ± 0.09	1.09 ± 0.09	0.88 ± 0.08	K	1999 Jul 17	1200
2MASSW J2208136+292121...	15.82 ± 0.09	14.83 ± 0.08	14.09 ± 0.08	1.73 ± 0.12	0.99 ± 0.12	0.74 ± 0.11	K	1998 Dec 24	2150
								1998 Dec 25	2400
2MASSW J2224438−015852...	14.05 ± 0.03	12.80 ± 0.03	12.02 ± 0.03	2.04 ± 0.04	1.25 ± 0.04	0.79 ± 0.04	K	1999 Jul 16	1200

[a] Source designations for 2MASS discoveries are given as "2MASx Jhhmmss[.]s±ddmmss." The "x" in the prefix depends on the catalog from which the object was taken; "P" is used for objects discovered in the prototype data, "SW" is used for objects taken from the actual working database of the survey, and "SI" is used for objects taken from one of the 2MASS incremental releases. The suffix conforms to IAU nomenclature convention and is the sexigesimal right ascension and declinaton at J2000.0 equinox.

[b] (K) Keck; (P) Palomar.

2. TARGET SELECTION AND SPECTROSCOPIC CONFIRMATION

In Paper I we searched for objects in the 2MASS data having $J - K_s \geq 1.30$, $K_s \leq 14.50$, and no optical counterpart. This technique proved efficient in finding L dwarfs but was most sensitive to the earliest types, since such a magnitude-limited search samples a much larger volume of space for early-type objects of higher luminosity than it does for late-type objects of lower luminosity. As a result, Paper I contained very few late L dwarfs. Also, because of the small initial survey area (only 371 deg^2) very few brighter, closer L dwarfs were identified. In this paper we address both deficiencies.

To find more examples of the latest L types, we have searched for 2MASS objects having $J - K_s \geq 1.7$, $K_s \leq 15.0$, and no optical counterpart on the POSS II plates. To find nearer examples of all L types, we have also searched for 2MASS objects having $J - K_s \geq 1.3$ and $K_s \leq 13.0$ and having either no POSS II counterpart or a counterpart implying colors of $R - K_s > 6$.

Spectroscopic follow-up of candidates selected with these search criteria have confirmed a few dozen new L dwarfs in the still-growing database. These are listed in Table 1, along with another dozen L dwarfs that met the same color criteria but were fainter at K_s. A final L dwarf with bright magnitudes but bluer colors ($J - K_s = 1.25$) is also included. In Table 1, column 1 lists the object name and columns 2–7 list the 2MASS-measured magnitudes and colors.

2.1. Keck Observations

Of the L dwarfs in Table 1, 65 were confirmed in 1998 August, 1998 December, 1999 March, and 1999 July using the Low Resolution Imaging Spectrograph (LRIS; Oke et al. 1995) at the 10 m W. M. Keck Observatory on Mauna Kea, Hawaii. A 400 line mm^{-1} grating blazed at 8500 Å was used with a 1″ slit and 2048 × 2048 CCD to produce 9 Å resolution spectra covering the range 6300–10100 Å. The OG570 order-blocking filter was used to eliminate second-order light. The data were reduced and calibrated using standard IRAF routines. A 1 s dark exposure was used to remove the bias, and quartz lamp flat-field exposures were used to normalize the response of the detector.

The individual stellar spectra were extracted using the APEXTRACT routine in IRAF, allowing for the slight curvature of a point-source spectrum viewed through the LRIS optics and using a template where necessary. Wavelength calibration was achieved using NeAr arc lamp exposures taken after each program object. Finally, the spectra were flux calibrated using observations of standards LTT 9491, Hiltner 600, LTT 1020, and Feige 56 from Hamuy et al. (1994). The data have not been corrected for telluric absorption, so the atmospheric O$_2$ bands at 6867–7000 and 7594–7685 Å and H$_2$O bands at 7186–7273, 8161–8282, ~8950–9300, and ~9300–9650 Å are still present in the spectra.
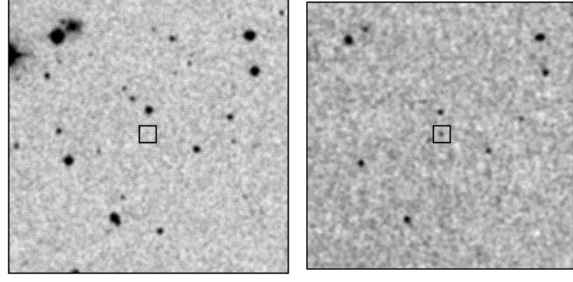
2.2. Palomar Observations

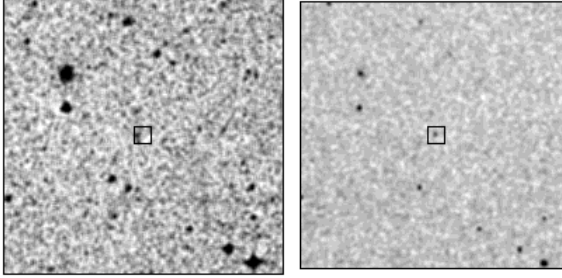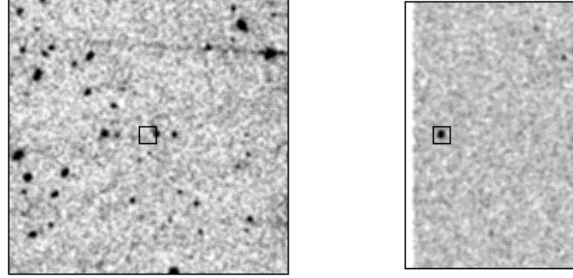The other two L dwarfs in Table 1 were confirmed using
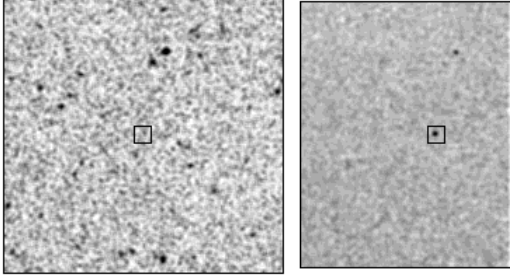
2MASSW J0015447+351603
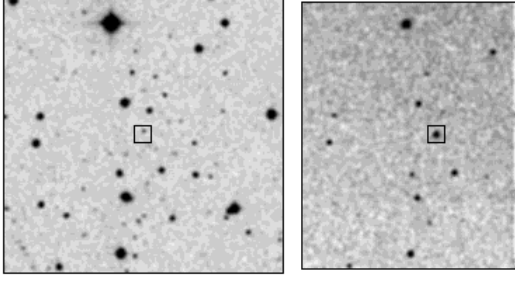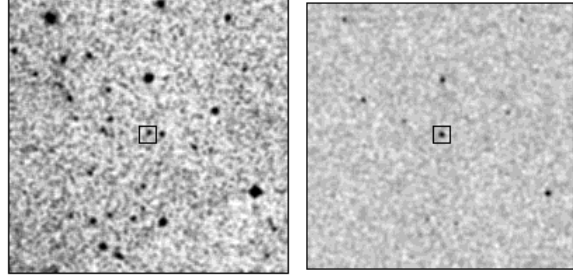
2MASSI J0028394+150141
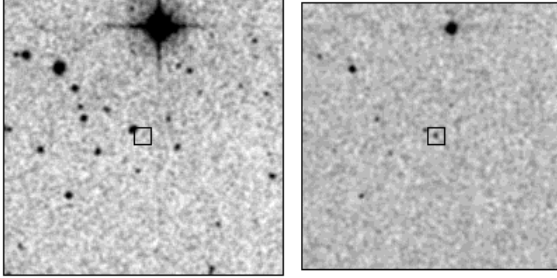
2MASSW J0030300−145033
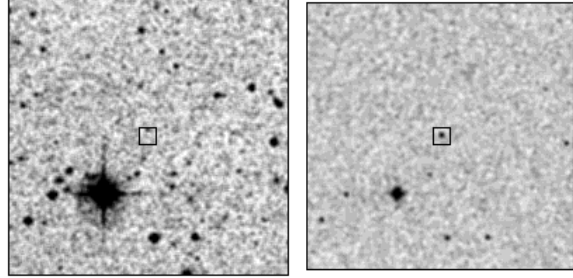
2MASSW J0036159+182110

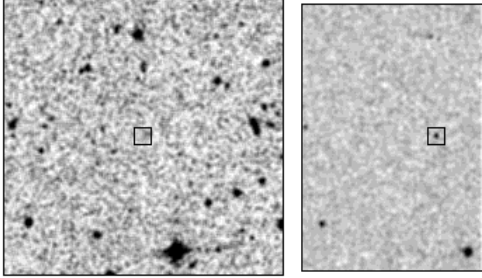## 2MASSW J0051107−154417

2MASSW J0058425−065123

2MASSI J0103320+193536

2MASSW J0135358+120522

2MASSW J0205034+125142
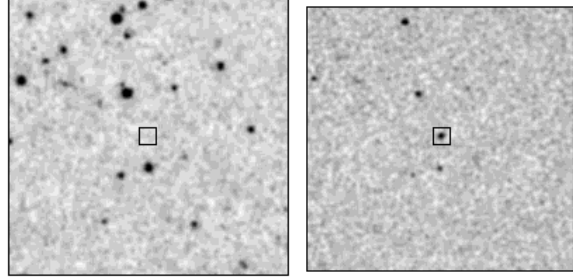
2MASSW J0208183+254253

FIG. 1.—Finder charts for each of the 67 L dwarfs listed in Table 1. For each object, two views are shown: the Digitized Sky Survey (DSS) image (*left*) and the 2MASS K_s image (*right*). Each view is to the same scale, 5′ on a side. North is up and east is to the left. The L dwarf is marked with a box on the 2MASS image, and a box at the same position is also shown on the DSS image. Note that the DSS image is centered on the position of the 2MASS object but that the 2MASS image does not always cover the full 5′ × 5′ field.

2MASSW J0208236+273740
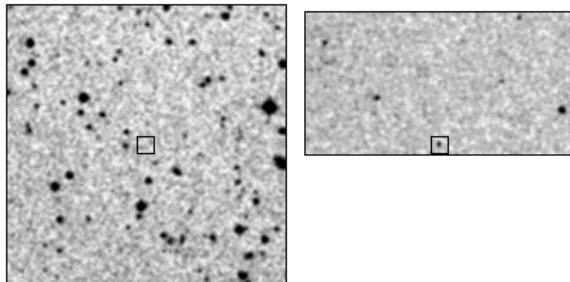
2MASSW J0208549+250048
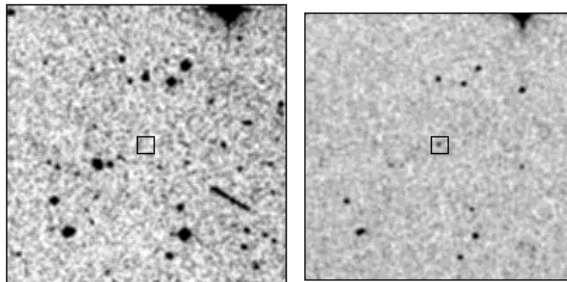
2MASSI J0224367+253704
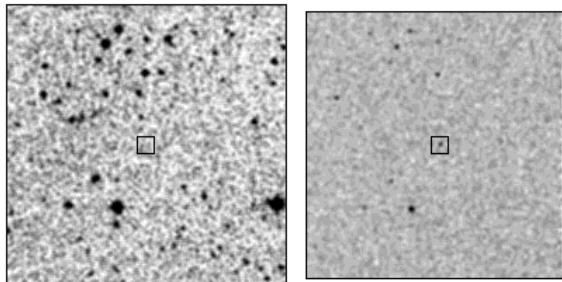
2MASSI J0302012+135814
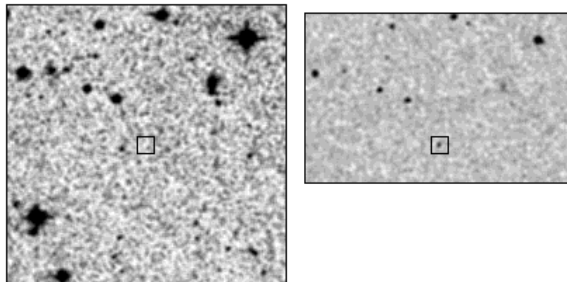
2MASSW J0306268+154514
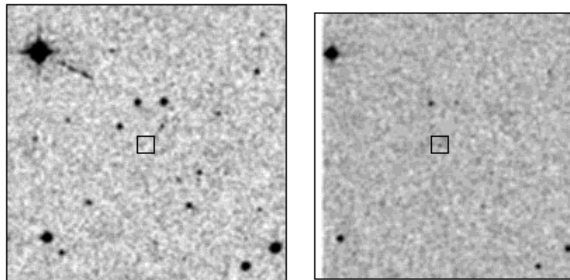
2MASSW J0309088−194938
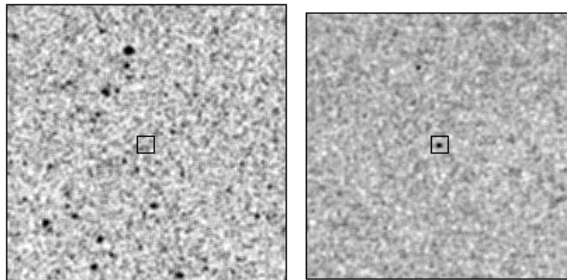
2MASSW J0310599+164816
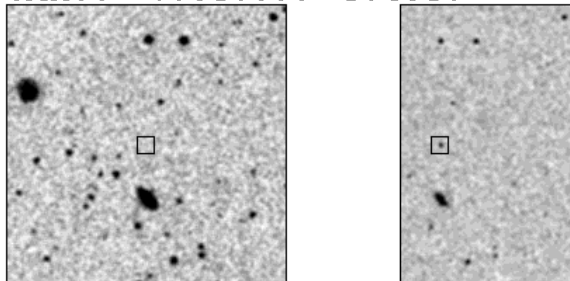
2MASSI J0328426+230205
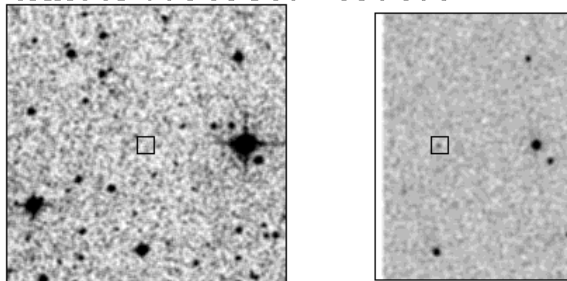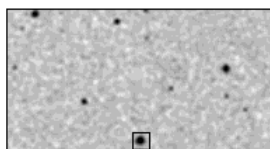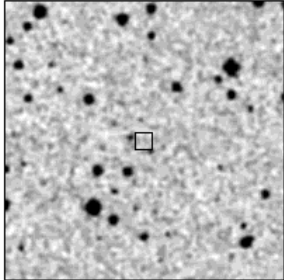
2MASSW J0337036−175807
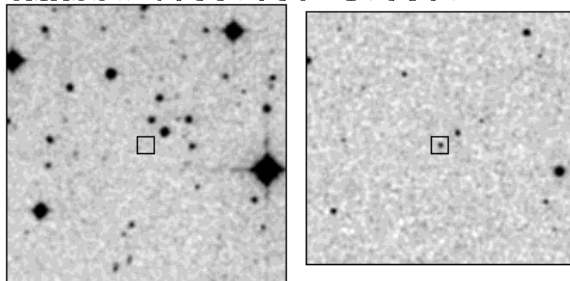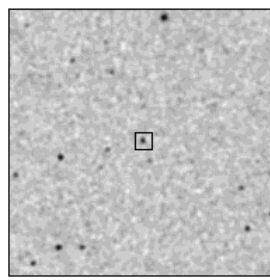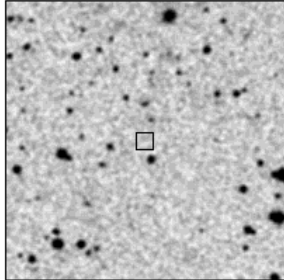
2MASSI J0409095+210439
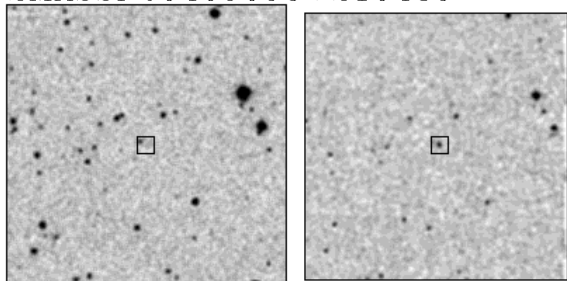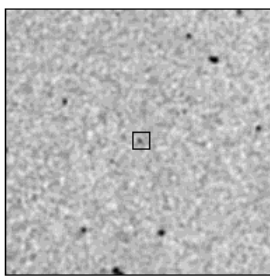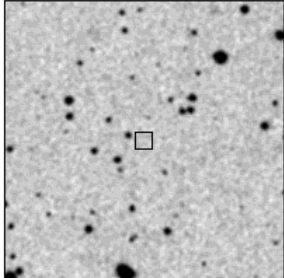
Fig. 1.—*Continued*

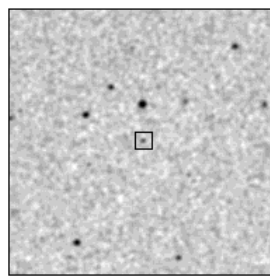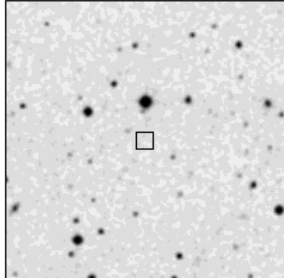## 2MASSW J0708213+295035
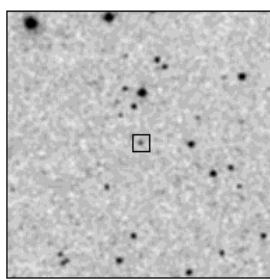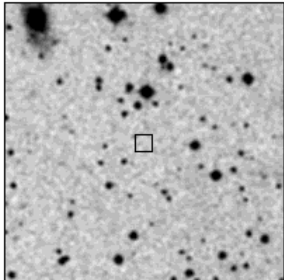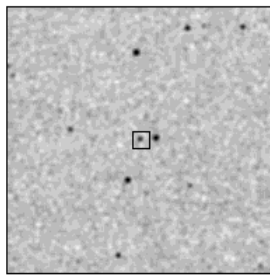
2MASSW J0740096+321203
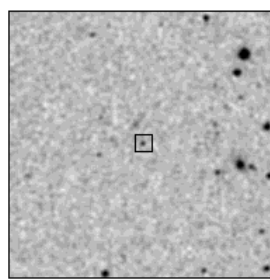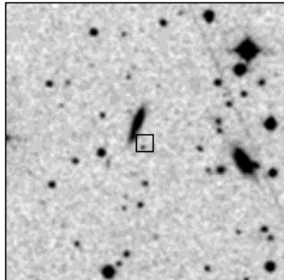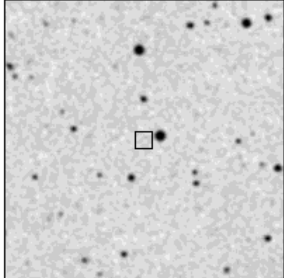
2MASSI J0746425+200032

2MASSI J0753321+291711
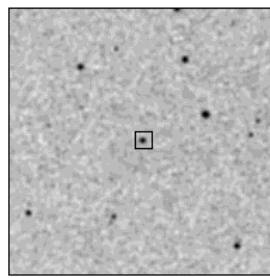
2MASSI J0756252+124456

2MASSW J0801405+462850

2MASSW J0820299+450031

2MASSI J0825196+211552
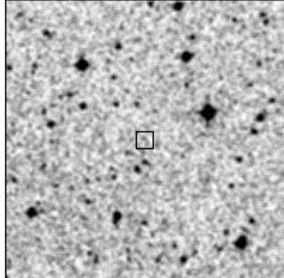
2MASSW J0829066+145622
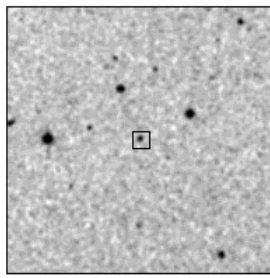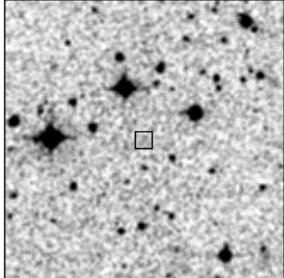
2MASSW J0829570+265510

Fig. 1.—*Continued*

452

2MASSW J0832045−012835
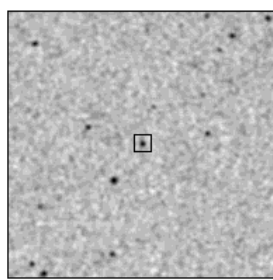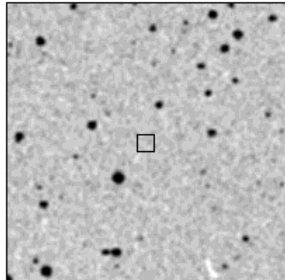
2MASSW J0920122+351742
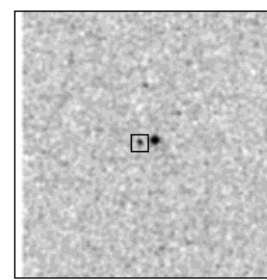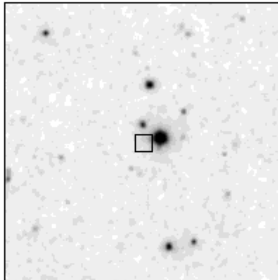
2MASSW J0928397−160312
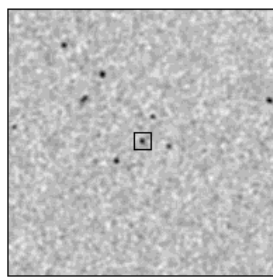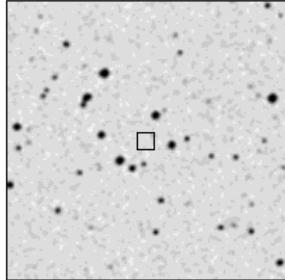
2MASSW J0929336+342952
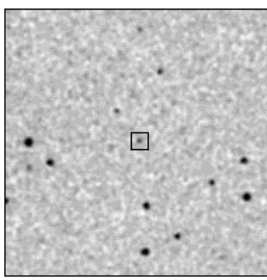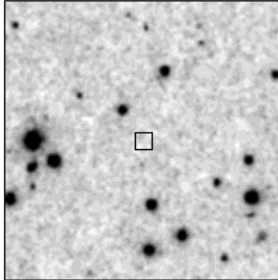
2MASSW J0944027+313132
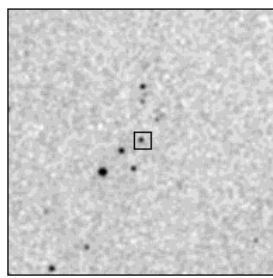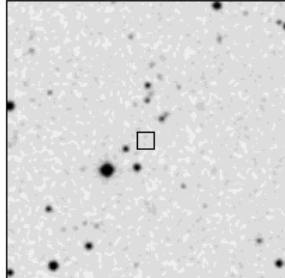
2MASSW J0951054+355801
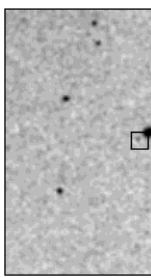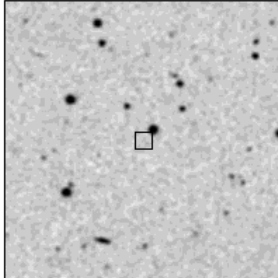
2MASSI J1029216+162652
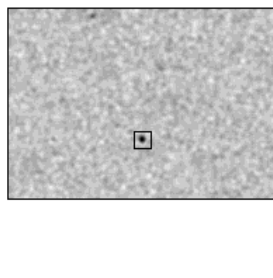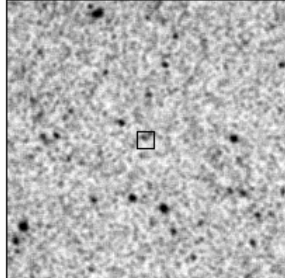
2MASSW J1035245+250745
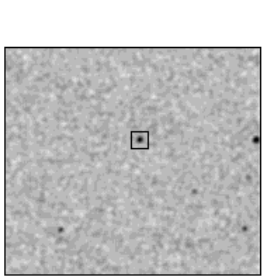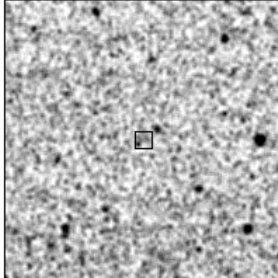
2MASSW J1102337−235945
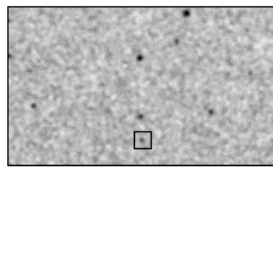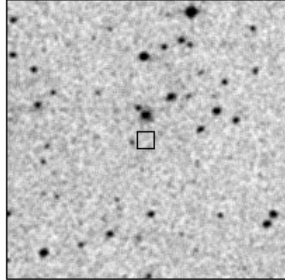
2MASSW J1112257+354813

FIG. 1.—*Continued*

453
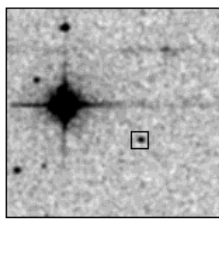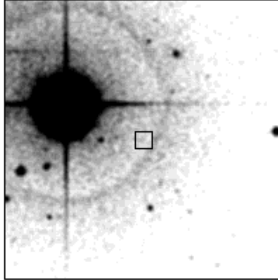
2MASSW J1123556+412228
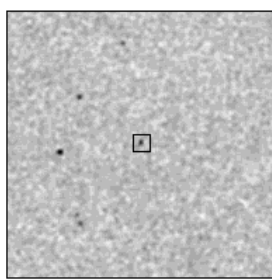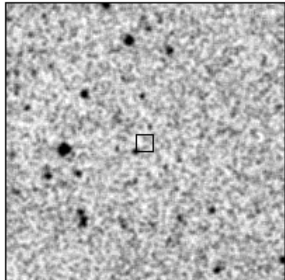
2MASSW J1239272+551537
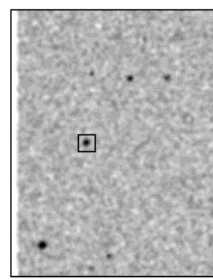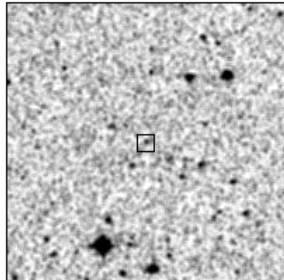
2MASSW J1246467+402715
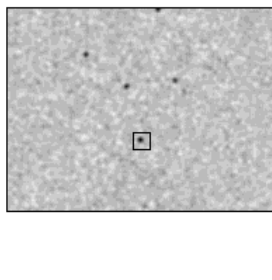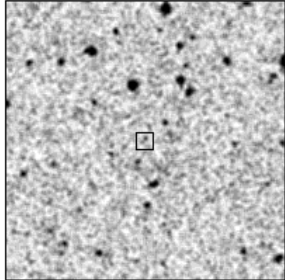
2MASSI J1332286+263508
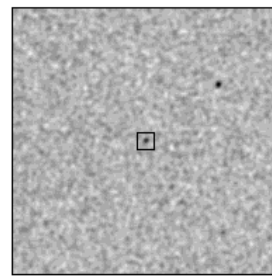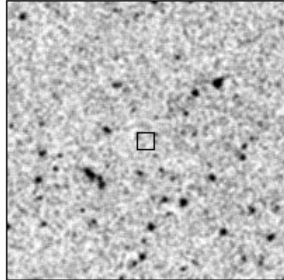
2MASSW J1338261+414034
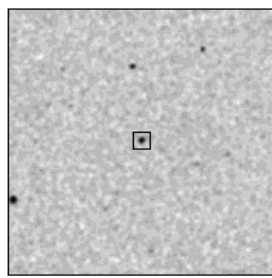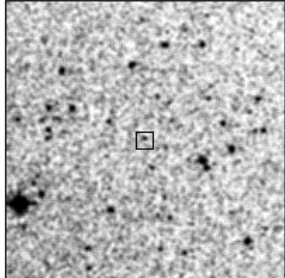
2MASSW J1343167+394508
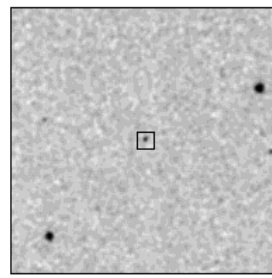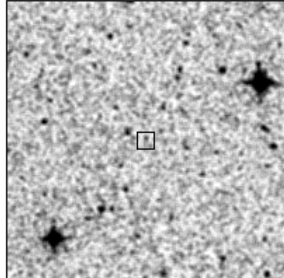
2MASSW J1411175+393636
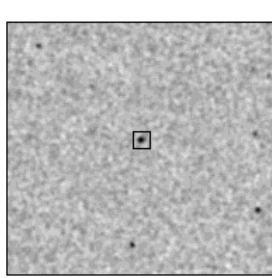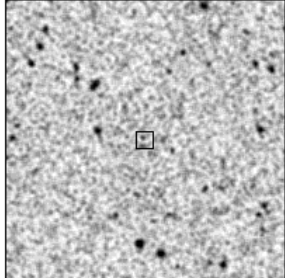
2MASSW J1412244+163312
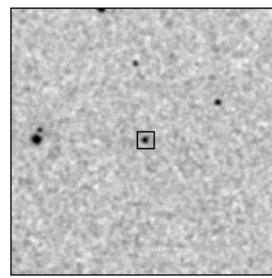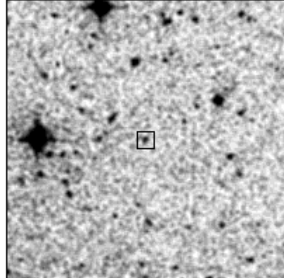
2MASSW J1438549−130910
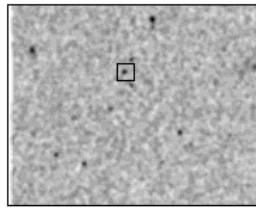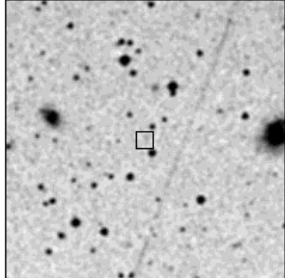
2MASSW J1449378+235537

Fig. 1.—*Continued*

454
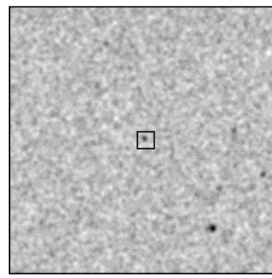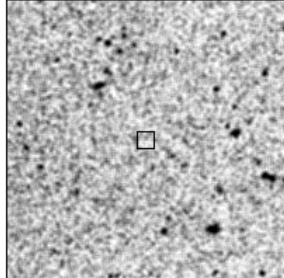
2MASSW J1507476−162738
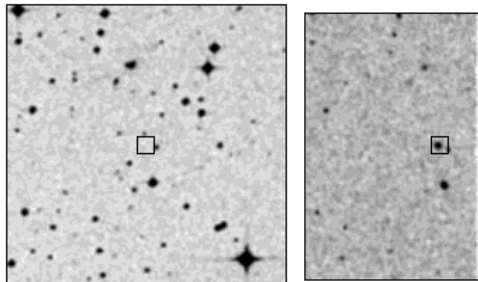
2MASSW J1523226+301456
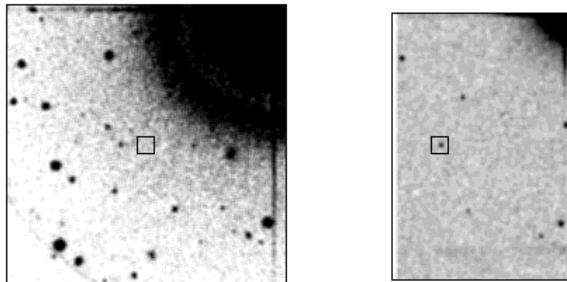
2MASSI J1526140+204341
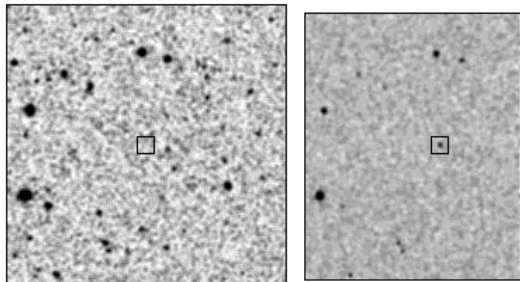
2MASSI J1600054+170832
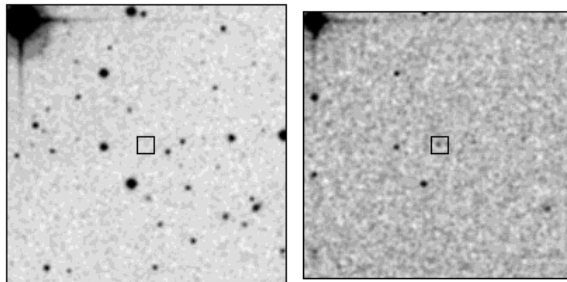
2MASSW J1615441+355900
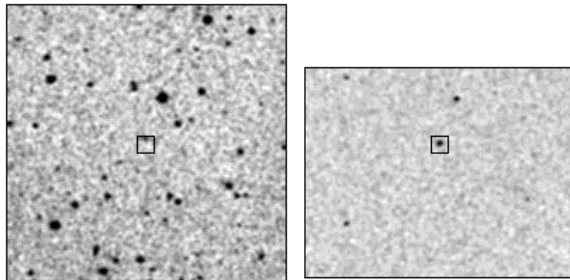
2MASSI J1656188+283506
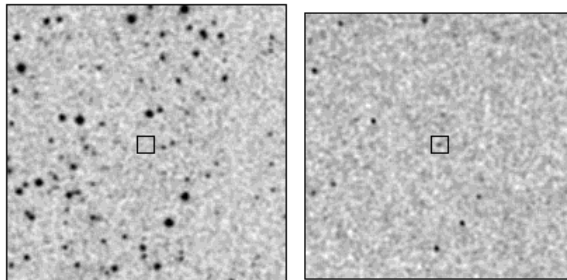
2MASSI J1711457+223204
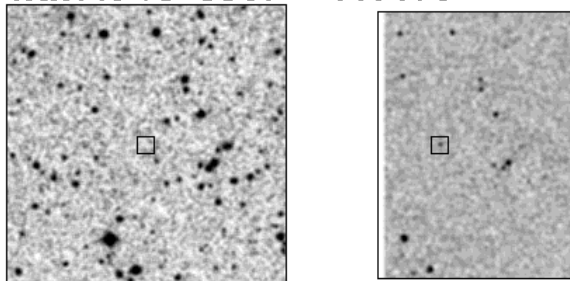
2MASSI J1726000+153819
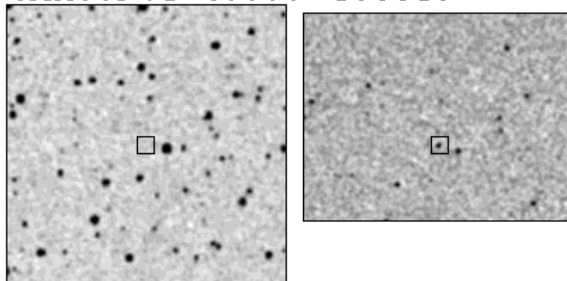
2MASSW J1728114+394859
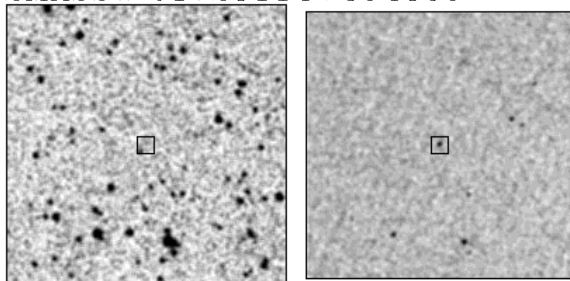
2MASSW J1743415+212707

Fig. 1.—*Continued*

455

2MASSW J1841086+311727

2MASSI J2054358+151904

2MASSI J2057153+171515

2MASSW J2101154+175658

2MASSW J2206450−421721

2MASSW J2208136+292121

2MASSW J2224438−015852
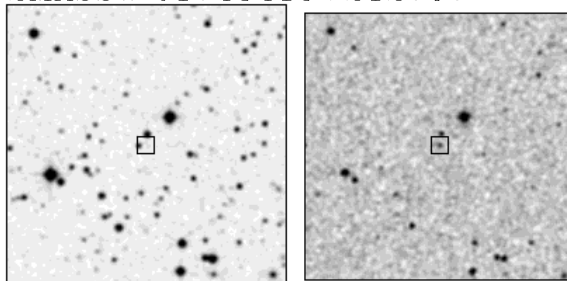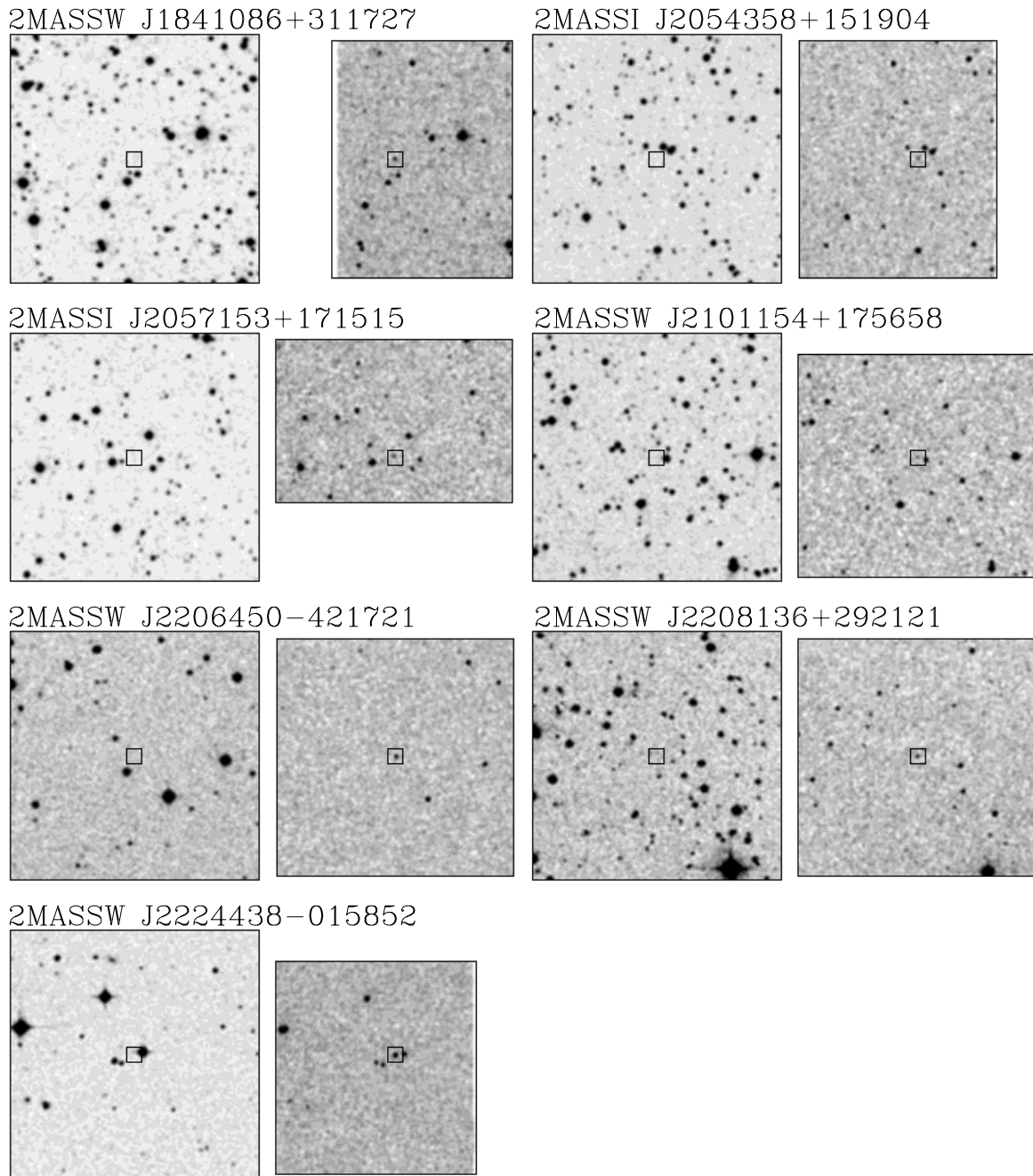
FIG. 1.—*Continued*

the Double Spectrograph (Oke & Gunn 1982) at the 5 m Hale Telescope on Palomar Mountain, California. A 2″.0 slit and dichroic beam splitter that splits the light near 6800 Å was used. A 316 line mm^{-1} grating was placed in the red camera for coverage from 6800 to 9150 Å at a resolution of 10 Å. A 300 line mm^{-1} grating was used in the blue camera to cover the range 3375 to 6825 Å, but neither of the L dwarfs had flux detected in the blue. Reductions were identical to those described for the Keck data above.

The telescope used for the spectroscopic observation of each target is listed in column 8 of Table 1, along with the observation date in column 9 and exposure time in column 10. Finding charts for each of these L dwarfs are shown in Figure 1.

3. SPECTROSCOPIC CLASSIFICATION

Spectral types were assigned following the guidelines

established in Paper I. The ratios CrH-*a*, Rb-*b*/TiO-*b*, Cs-*a*/VO-*b*, and Color-*d* ratios, as defined in Paper I, were measured from each spectrum. These are tabulated in columns 2–5 of Table 2, where the names of the L dwarfs are listed in column 1. The values in parentheses after the measured value of each ratio are the class or range in class that most closely corresponds to that value, as judged from the primary standards plotted in Figures 10–12 of Paper I. For those spectra whose ratios suggest a type earlier that L5, we have listed in column 6 the spectral class of the primary spectrum that best fits the K I profile. These primary spectra are the ones listed in Table 6 of Paper I. The types implied by the three CrH-*a*, Rb-*b*/TiO-*b*, and Cs-*a*/VO-*b* ratios, along with the type implied by either the Color-*d* ratio (for types later than L5) or the K I fit (for types ≤L5) have been medianed to produce the final spectral type.

This procedure works well except for spectra with lower

L. Dwarf (1)	CrH-*a* (2)	Rb-*b*/TiO-*b* (3)	Cs-*a*/VO-*b* (4)	Color-*d* (5)	K I Fit (6)	Oxide Fit (7)	Sp. T. (8)	Hα EW (Å) (9)	Li I EW (Å) (10)	Est. Dist. (pc) (11)
2MASSW J0015447+351603...	1.47 (1–2)	1.07 (2)	0.97 (2)	5.77 (–)	(2)		L2 V	2	<0.5	20
2MASSI J0028394+150141	2.84 (5)			10.38 (5)	(4)	(5)	L4.5 V	<2	<5	45
2MASSW J0030300−145033...	1.62 (7)			14.23 (5)		(8)	L7 V	<10	<5	28
2MASSW J0036159+182110...	1.72 (3–4)	1.16 (3)	1.12 (3)	8.73 (–)	(3–4)		L3.5 V	<0.5	<0.5	8.7[a]
2MASSW J0051107−154417...	1.57 (2)	1.43 (4–5)	1.06 (2–3)	8.62 (–)	(4)		L3.5 V	<2	10	30
2MASSW J0058425−065123...	1.16 (0)	0.73 (0)	0.74 (M9)	6.53 (–)	(0)		L0 V	2	<1	32
2MASSI J0103320+193536...	1.96 (5–6)	2.05 (7)	1.47 (5)	16.36 (6)			L6 V	<1	12	29
2MASSW J0135358+120522...	1.39 (1)	1.01 (1–2)	0.93 (1–2)	5.76 (–)	(2)		L1.5 V	7	<0.5	28
2MASSW J0205034+125142...	2.19 (5)	1.93 (6–7)	1.24 (4)	10.95 (5)	(4–5)		L5 V	<1	<1	27
2MASSW J0208183+254253...	1.37 (1)	0.86 (1)	0.87 (1)	6.52 (–)	(2)		L1 V	<0.5	<0.5	25
2MASSW J0208236+273740...	2.14 (5)	1.41 (4)	1.57 (6–7)	10.66 (5)	(4–5)		L5 V	<1	<1	29
2MASSW J0208549+250048...	1.89 (4)	1.51 (4–5)	1.72 (8+)	11.61 (5)	(5)		L5 V	<1	12	36
2MASSI J0224367+253704	1.56 (2)	1.08 (2)	1.21 (3–4)	6.19 (–)	(2)		L2 V	<1	<1	66
2MASSI J0302012+135814	1.81 (4)	1.13 (3)	1.11 (3)	6.68 (–)	(2)		L3 V	<2	5	56
2MASSW J0306268+154514...	1.59 (7)			13.88 (5)		(6–8)	L6: V	<6	<6	44
2MASSW J0309088−194938...	1.72 (3)			11.54 (5)	(4)	(5)	L4.5 V	<7	<6	34
2MASSW J0310599+164816...	1.24 (8)			31.55 (8)	(8+)	(8+)	L8 V	<3	5	20
2MASSI J0328426+230205	1.16 (8+)			31.21 (8)	(8+)	(8+)	L8 V	<4	<3	24
2MASSW J0337036−175807...	1.62 (3)			11.33 (5)	(4–5)	(5)	L4.5 V	<5	8	29
2MASSI J0409095+210439	1.67 (3)	1.10 (2–3)	1.21 (3–4)	7.71 (–)	(3)		L3 V	<1	<2	38
2MASSW J0708213+295035...	2.18 (5)			13.00 (5)	(5)	(5–6)	L5 V	<2	<5	44
2MASSW J0740096+321203...	2.46 (5)	1.54 (4–5)	1.38 (4–5)	10.13 (5)	(4)		L4.5 V	<2	<2	37
2MASSI J0746425+200032	1.29 (0–1)	0.74 (0–1)	0.88 (1)	6.41 (–)	(0–1)		L0.5 V	2	<0.5	12.3[a]
2MASSI J0753321+291711	1.50 (2)	1.02 (2)	1.16 (3)	6.33 (–)	(2)		L2 V	<0.5	<1	42
2MASSI J0756252+124456	1.47 (7–8)			15.19 (6)		(5)	L6 V	<3	15	35
2MASSW J0801405+462850...	1.62 (7)	1.87 (6)	1.82 (8+)	13.03 (5)			L6.5 V	<2	<2	28
2MASSW J0820299+450031...	2.38 (5)	1.63 (5–6)	1.54 (6)	11.76 (5)	(4)		L5 V	<2	<4	36
2MASSI J0825196+211552	1.44 (7–8)	2.10 (7)	1.43 (5)	25.22 (7–8)			L7.5 V	<2	10	12
2MASSW J0829066+145622...	1.58 (2)	1.01 (2)	1.08 (3)	5.70 (–)	(2)		L2 V	<0.5	<0.5	30
2MASSW J0829570+265510...	2.13 (5)			17.72 (6–7)		(7)	L6.5 V	<10	18	37
2MASSW J0832045−012835...	1.46 (1–2)	1.00 (2)	0.90 (1–2)	6.58 (–)	(2)		L1.5 V	2	<1	25
2MASSW J0920122+351742...	1.68 (6–7)	1.84 (6)	1.72 (8+)	20.61 (7)			L6.5 V	<0.5	<0.5	21
2MASSW J0928397−160312...	1.54 (2)	1.11 (2–3)	1.03 (2)	5.90 (–)	(2)		L2 V	<0.5	<1	39
2MASSW J0929336+342952...	1.22 (8)			22.39 (7)		(8)	L8 V	<3	≤11	22
2MASSW J0944027+313132...	1.58 (2)	1.07 (2)	0.89 (1–2)	6.65 (–)	(2)		L2 V	≤1	<1	44
2MASSW J0951054+355801...	1.67 (3)			15.94 (6)		(6–7)	L6 V	<5	<10	45
2MASSI J1029216+162652	1.72 (3–4)	1.08 (2)	1.03 (2)	6.86 (–)	(2–3)		L2.5 V	0.5	<0.5	23
2MASSI J1035245+250745	1.41 (4)	0.88 (1)	0.87 (1)	6.15 (–)	(1–2)		L1 V	<1	<1	35
2MASSW J1102337−235945...	1.35 (1:)			9.03 (–)	(4)	(5)	L4.5 V	<5	≤5	53
2MASSW J1112257+354813...	1.98 (5)	1.60 (5)	1.28 (4)	9.90 (–)	(4)		L4.5 V	≤1	9	21.7[a]
2MASSW J1123556+412228...	1.55 (2)	1.16 (3)	1.03 (2)	5.91 (–)	(2)		L2.5 V	<1	<1	51
2MASSW J1239272+551537...	2.05 (5)	1.71 (5–6)	1.40 (5)	11.45 (5)	(4–5)		L5 V	<3	14	17
2MASSW J1246467+402715...	1.85 (4)	1.30 (4)	1.39 (4–5)	9.43 (–)	(4)		L4 V	≤1	11	25
2MASSI J1332286+263508	1.49 (2)	1.06 (2)	1.02 (2)	5.92 (–)	(2)		L2 V	<2	<2	55
2MASSI J1338261+414034...	1.54 (2)	1.06 (2)	1.07 (2–3)	7.05 (–)	(3)		L2.5 V	≤1	<0.5	23
2MASSW J1343167+394508...	2.36 (5)	1.77 (6)	1.48 (5)	13.03 (5)	(4–5)		L5 V	<3	≤20	34
2MASSW J1411175+393636...	1.35 (1)	0.99 (2)	0.84 (1)	6.88 (–)	(2)		L1.5 V	<1	<1	33
2MASSI J1412244+163312...	1.27 (0–1)	0.79 (1)	0.79 (0–1)	6.23 (–)	(0)		L0.5 V	4	<0.5	26
2MASSW J1438549−130910...	1.50 (2)			6.93 (–)	(2–3)	(~4)	L3: V	<4	<4	38
2MASSW J1449378+235537...	1.18 (0)				(0)	(0)	L0 V		<10	62
2MASSW J1507476−162738...	1.99 (5)	1.46 (4–5)	1.39 (4–5)	13.19 (5)	(5)		L5 V	<0.5	<0.5	8:[a]
2MASSW J1523226+301456...	1.19 (8+)			35.16 (8+)		(8)	L8 V	<15	9	18.6[a]
2MASSI J1526140+204341	1.91 (6)	2.43 (7–8)	2.16 (8+)				L7 V		<10	19
2MASSI J1600054+170832	1.57 (2)	0.72 (0)	0.91 (1–2)	6.94 (–)	(2)		L1.5 V	<1.5	<2	62
2MASSW J1615441+355900...	1.86 (4)	1.02 (2)	1.15 (3)	7.68 (–)	(3)		L3 V	<1	<1	24
2MASSI J1656188+283506	1.75 (3–4)			10.74 (5)	(4)	(5)	L4.5 V	<6	<3	56
2MASSI J1711457+223204	1.96 (5–6)			16.87 (6–7)		(6–7)	L6.5 V	<4	≤7	36
2MASSI J1726000+153819	1.44 (1–2)	1.31 (4)	0.93 (1–2)	8.44 (–)	(2)		L2 V	<2	6	42
2MASSW J1728114+394859...	1.52 (7)			19.76 (7)		(7)	L7 V	<7	<4	20
2MASSW J1743415+212707...	1.49 (2)	1.31 (4)	0.99 (2)	5.84 (–)	(3)		L2.5 V	6	<1	42
2MASSW J1841086+311727...	1.41 (1)	1.06 (2)	1.10 (3)	5.04 (–)	(2?)		L4 V pec[b]	<2	<2	40
2MASSI J2054358+151904	1.04 (M9)			5.38 (–)	(0)	(2–3)	L1: V	<6	<4	75
2MASSI J2057153+171515	1.44 (1–2)	0.93 (1–2)	0.83 (0–1)	5.61 (–)	(2)		L1.5 V	<2	<1	61
2MASSW J2101154+175658...	2.09 (5–6)			27.61 (7–8)		(7–8)	L7.5 V	<7	<5	29
2MASSW J2206540−421721...	1.26 (0–1)	1.39 (4)	1.03 (2)	6.75 (–)	(2)		L2 V	≤2	8	41
2MASSW J2208136+292121...	1.32 (1)	0.98 (2)	1.06 (2–3)	6.73 (–)	(0 pec)		L2 V pec[c]	<2	4	48
2MASSW J2224438−015852...	1.99 (5)	1.56 (4–5)	1.20 (3–4)	10.71 (5)	(4–5)		L4.5 V	1	<0.5	14

[a] Distances determined via trigonometric parallax. See text and Table 3 for details.

[b] This object has a peculiar spectrum showing feature strengths that match those of an L4 dwarf, although the overall color between 6300 and 10000 Å is too blue for the object to be even early L.

[c] This object has a peculiar spectrum showing narrow K I lines like that of an L0 dwarf but TiO bands with strengths similiar to an L4 dwarf.
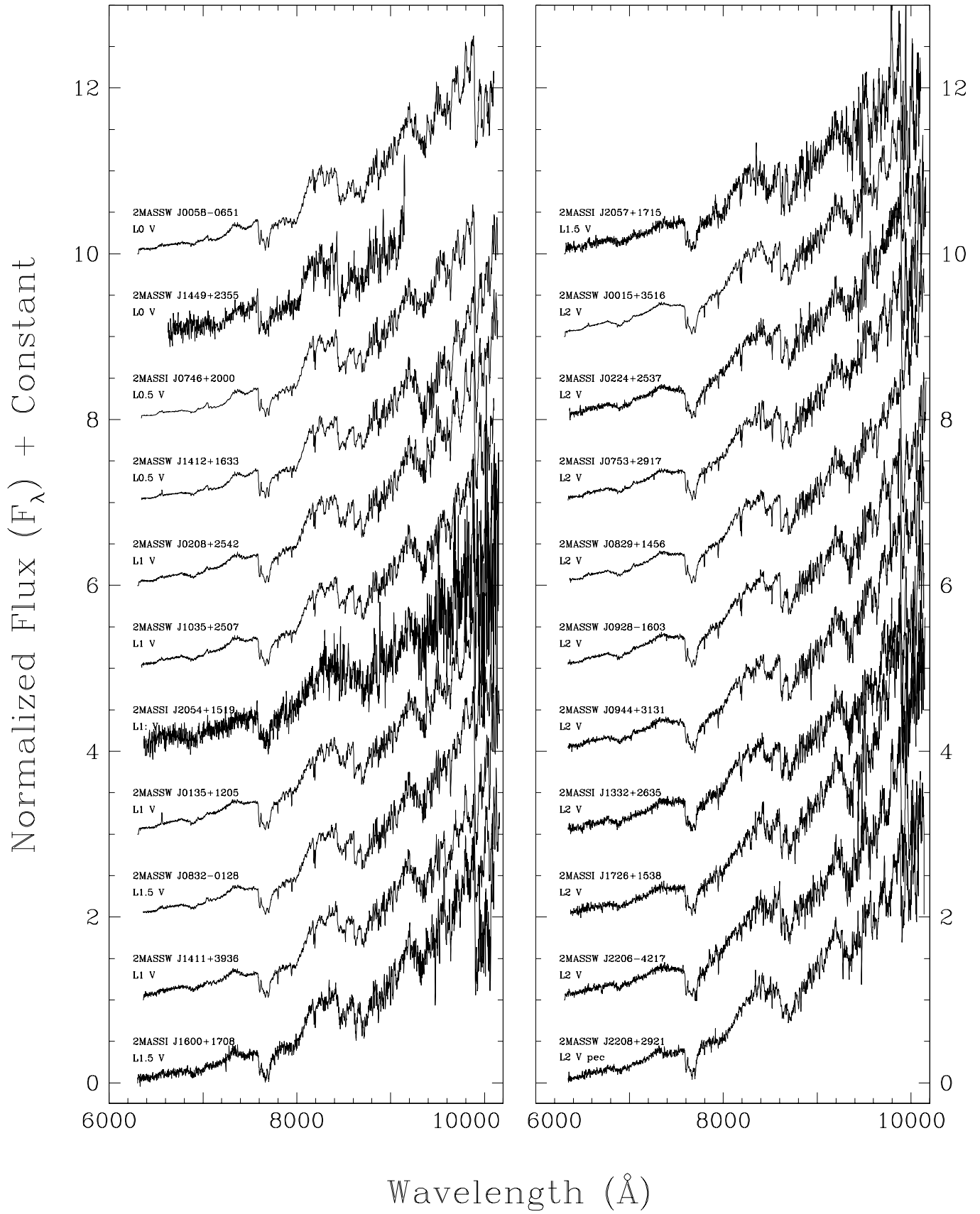
FIG. 2.—Spectra of all 67 new L dwarfs. The flux scale is in units of F_λ, normalized to 1 at 8250 Å. Integral offsets have been added to the flux scale to separate the spectra vertically. Names for the 2MASS objects have been abbreviated.

FIG. 2.—*Continued*

459

Y-axis: Normalized Flux (F_λ) + Constant

X-axis: Wavelength (Å)

Left panel labels (top to bottom):
2MASSW J0208+2500 L5 V
2MASSW J0708+2950 L5 V
2MASSW J0820+4500 L5 V
2MASSW J1239+5515 L5 V
2MASSW J1343+3945 L5 V
2MASSW J1507−1627 L5 V
2MASSI J0103+1935 L6 V
2MASSW J0306+1545 L6: V
2MASSI J0756+1244 L6 V
2MASSW J0951+3558 L6 V
2MASSW J0801+4628 L6.5 V

Right panel labels (top to bottom):
2MASSW J0829+2655 L6.5 V
2MASSW J0920+3517 L6.5 V
2MASSI J1711+2232 L6.5 V
2MASSW J0030−1450 L7 V
2MASSI J1526+2043 L7 V
2MASSW J1728+3948 L7 V
2MASSI J0825+2115 L7.5 V
2MASSW J2101+1756 L7.5 V
2MASSW J0929+3429 L8 V
2MASSI J0328+2302 L8 V
2MASSW J0310+1648 L8 V
2MASSW J1523+3014 L8 V

FIG. 2.—*Continued*

FIG. 3.—Spectral ratios vs. spectral subclass for the new L dwarfs from this paper (Table 2), together with the 25 L dwarfs from Paper I: (a) CrH-a, (b) Rb-b/TiO-b, (c) Cs-a/VO-b, and (d) Color-d. The primary standards from Paper I are shown as large circles; new objects from this paper are shown as small circles. The spectra with lower signal-to-noise ratios are shown as crosses in (a) and (d).

signal-to-noise ratios. In these spectra, the narrower indices (Rb-b/TiO-b and Cs-a/VO-b) are more prone to uncertainties due to random noise spikes. For such cases, a comparison by eye with the alkali and oxide features of the primary standards is a more reliable indicator of type. Specifically, there are 21 lower quality spectra in Table 2 where the Rb-b/TiO-b and Cs-a/VO-b ratios have been replaced by the best fit to the 7800–8600 Å region encompassing the Rb I doublet, the Cs I λ8521 line, the VO band near 7900 Å, and the TiO band at 8432 Å. These best fits are listed in column 7 of Table 2.

Final spectral types for each object are listed in column 8 of Table 2. The 67 new L dwarf spectra are displayed in order of increasing L subtype in Figure 2. Values of the spectral ratios as a function of final spectral class are illustrated in Figure 3 with values for the 25 L dwarfs from Paper I shown for comparison.

4. SPECTROSCOPIC ANALYSES

The sample in Table 2 not only represents a huge increase in the number of L dwarfs known in general, but it also includes another 17 dwarfs with types of L6 or later. This larger sample can be used to study trends that evolve with spectral type.

4.1. Hα Emission

The absence of Hα emission in late L dwarfs, as hinted at in Paper I, can now be reinvestigated. Column 9 of Table 2 lists for all 67 spectra the measure of (or upper limit to) the equivalent width of the Hα emission feature. Detailed spectra near Hα are shown in Figure 4 for those objects exhibiting emission or possible emission. Figure 5a shows these equivalent widths as a function of spectral subclass. To provide a larger sample, the 25 L dwarfs from Paper I

have also been included. As the figure shows, typical Hα strengths for those early L dwarfs with emission are generally a few angstroms. Hα lines of similar strength would be detectable for several of the late L dwarfs here, but none shows the line. In fact, the latest L dwarf with detected Hα emission is the L4.5 dwarf 2MASSW J2224438−015852, and here the 1 Å equivalent-width line is observable only because of the spectacular signal-to-noise ratio in this spectrum.

Figure 5b shows as a function of L subclass the percentage of L dwarfs having Hα emission. Only those spectra with sufficient signal-to-noise ratio to enable detection of a line of equivalent width 2 Å are included in the computation. For type L0, 60% show Hα emission of this strength, but the percentage drops markedly for types L1, L2, and L3. For types L4 and L5, Hα emission is not detected at 2 Å equivalent width or greater in any of our sample. For many of the latest L dwarfs (L6–L8) the signal-to-noise ratio is too poor to exclude Hα emission at 2 Å equivalent width because our ability to detect low-level Hα emission is compromised by the paucity of red photons. That having been stated, even for those few L6–L8 dwarfs having sufficient signal-to-noise ratio, Hα emission was not detected either.

It should also be noted that Hα strengths for the entire ensemble of Hα-emitting L dwarfs are smaller than in typical dMe stars. Both this and the absence of measurable Hα in mid– and late L dwarfs indicate a decline in chromospheric activity throughout the L dwarf sequence. Gizis et al. (2000) have used the available data on L dwarfs with and without Hα emission to conclude that lack of activity may correlate with youth and substellar nature. Such a correlation would explain why Hα emission is not seen in dwarfs later than L4.5, as this subclass corresponds roughly to the temperature at which stellar interior models predict a substellar fraction of 100%. In other words, a mixture of stars
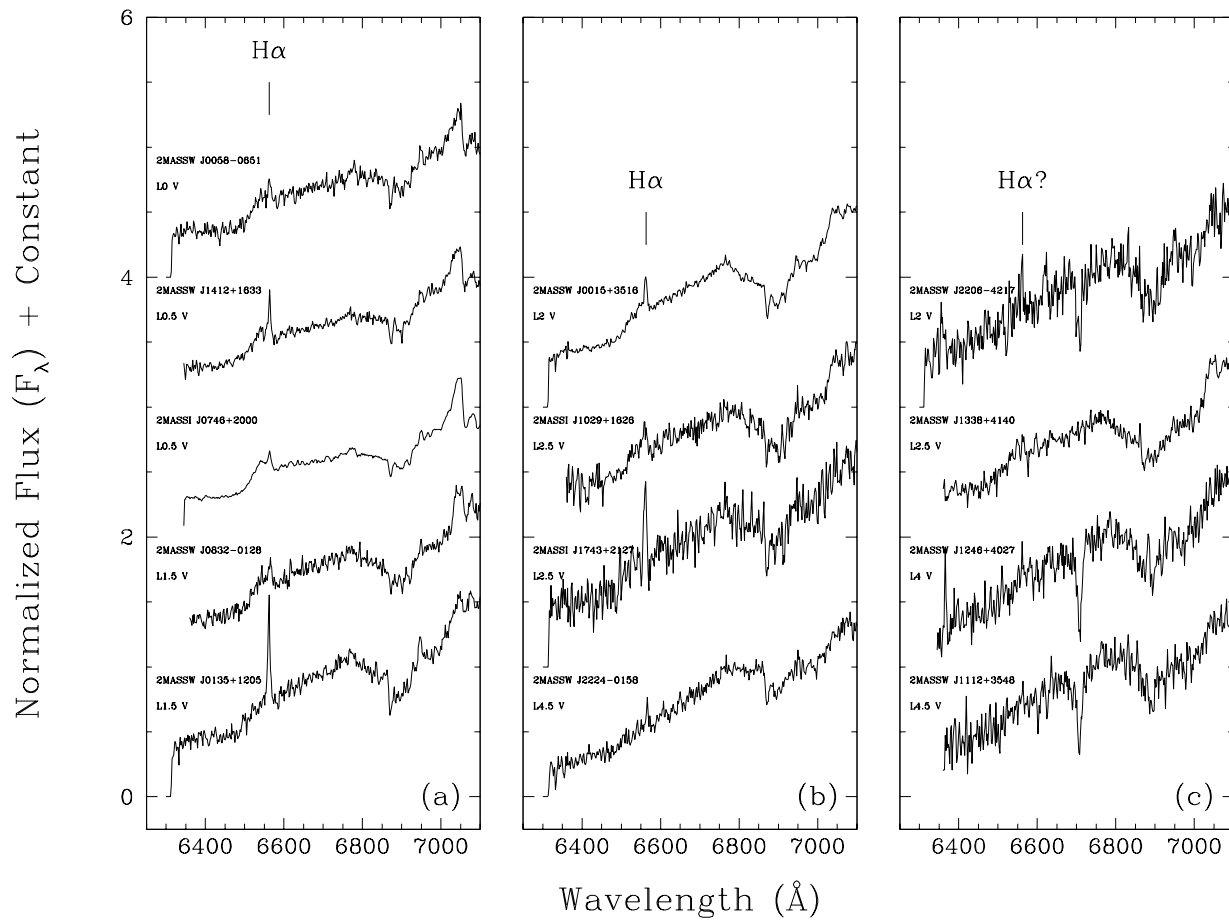
FIG. 4.—(a–b) Detailed spectra of nine new L dwarfs showing Hα emission. (c) Detailed spectra of another four new L dwarfs showing possible Hα emission at our limit of detectability.

and brown dwarfs is expected at earlier L types (where Hα emitters and non-Hα emitters lie), but later than this (types for which no Hα emitters are found), all objects are expected to be substellar. The seeming anticorrelation between L dwarfs with lithium absorption and those with Hα emission is more evidence in favor of this conclusion.

4.2. Lithium Absorption

Paper I also suggested that lithium disappears (or is much weaker) in the latest L dwarfs, probably because of the formation of lithium-bearing molecules (Burrows & Sharp 1999; Lodders 1999). We can reinvestigate this hypothesis also. Column 10 of Table 2 lists for each spectrum the measure of (or upper limit to) the equivalent width of the Li I doublet. Detailed spectra near the lithium doublet are shown in Figure 6 for those objects exhibiting Li absorption or possible absorption. Figure 7a shows these equivalent widths as a function of spectral subclass, and L dwarfs from Paper I have been added to increase the sample size.

For early and mid–L dwarfs with detected lithium, the equivalent width increases with later subclasses. This is the same behavior seen with the ground-state doublets of the other abundant alkalis Na I and K I. In these objects the cooler temperatures mean that more and more of the alkali atoms are in their neutral state. This effect, along with the pressure broadening and the increased column density through which the emergent radiation passes (thanks to an

atmosphere made more transparent by the removal of overlying TiO and VO absorption), creates stronger and stronger absorption lines. The main difference is that the lower cosmic abundance of lithium precludes the development of giant absorption troughs such as those produced by sodium and potassium (Reid et al. 2000).

However, the trend of increasing line strength for lithium, unlike sodium and potassium, reverses at types near L6.5–L7 V. Figure 7b shows the percentage of L dwarfs with detectable lithium as a function of spectral subclass. Only those L dwarfs with sufficient signal to see a line of 4 Å equivalent width are used in the calculation. The percentage of L dwarfs with strong lithium may drop for types L7 and L8 (although our statistics are still poor), but, as shown in Figure 7c, the strength of the line when detected is much weaker than that seen for types L5 and L6. In other words, although lithium is sometimes seen in the latest L dwarfs, its strength is greatly diminished. At face value, this seems to run contrary to the expectation that the latest L dwarfs should show increased line strengths of ground state Li I because of their cooler temperatures.

We interpret this as evidence for Li depletion due to the formation of lithium-bearing molecules. At temperatures typical of late M dwarfs, the primary lithium-bearing gas is Li. At cooler temperatures, however, lithium will begin to form molecules such as LiOH, LiCl, or LiF depending upon the physics of the gas mixture. Lodders (1999) concludes that at the pressures expected in these objects, LiCl is the
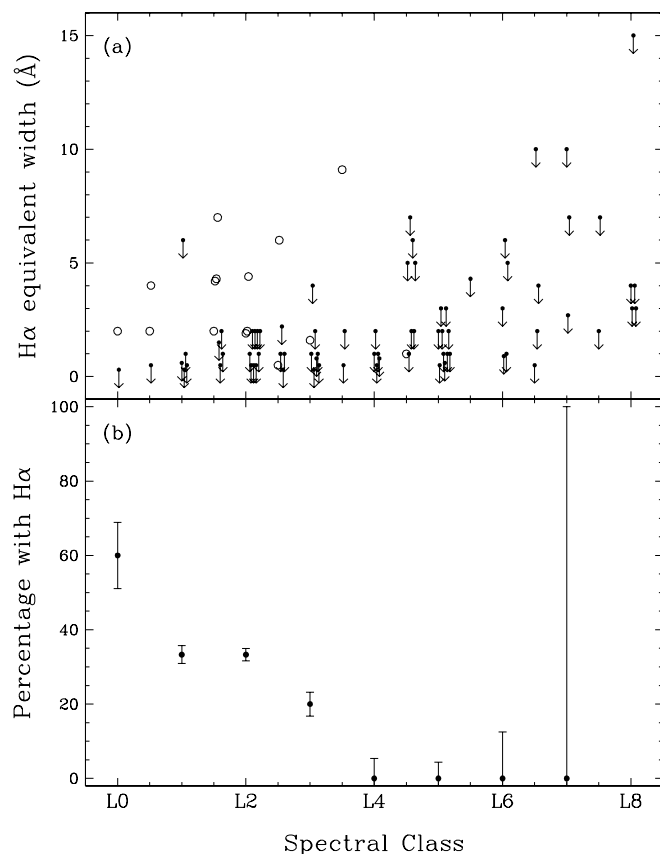
FIG. 5.—(a) Hα equivalent widths as a function of spectral subclass for the 67 L dwarfs from this paper and the 25 L dwarfs from Paper I. Open circles denote objects having a detected Hα emission line. Downward arrows denote upper limits to the Hα EW for those objects for which no line was detected. To display the data more clearly, some of the points have been given slight offsets along the x-axis. (b) Percentage of L dwarfs showing Hα emission as a function of spectral subclass. The only objects used in this computation are those for which an Hα equivalent width of 2 Å or more would be detectable. Points have been binned into integer sub-types in which L0 and L0.5 dwarfs have been combined in the L0 bin, L1 and L1.5 dwarfs have been combined in the L1 bin, etc.

molecule responsible for robbing Li out of the atmosphere. She also shows that Li and LiCl should have equal abundances near 1500–1550 K, with LiCl being dominant at cooler temperatures. Because dwarfs of type L6.5–L7 show clear signs of Li depletion in their spectra, we can conclude that such dwarfs have temperatures in the 1500 K realm. A more robust temperature estimate would require observations of a band of LiCl so that abundances of Li and LiCl could be directly compared.

5. DISTANCES

In addition to increasing the sample size of L dwarfs, particularly at the latest types, another goal of our survey was to find nearer examples of all L types. A few of the brighter objects in Table 2 already have measured trigonometric parallaxes, a couple of which are within 10 pc of the Sun. We can use these parallaxes as well as other parallaxes from D. Dahn (2000, private communication) and from the literature to estimate distances to the rest. Shown in Figure 8 are plots of absolute J magnitude and absolute K_s magnitude as a function of spectral class for late M, L, and T dwarfs. The objects plotted here are listed in Table 3, where

the object name and spectral type are listed in columns 1–2, the reference for the trigonometric parallax measure is listed in column 3, and M_J and M_{K_s} values (derived from 2MASS J and K_s photometry) are listed in columns 4 and 5, respectively.

A second-order least-squares fit to the late M and L dwarfs gives the following relations between absolute magnitude and spectral class:

$$M_J = 11.780 + 0.198(\text{subclass}) + 0.023(\text{subclass})^2 , \quad (1)$$

$$M_{K_s} = 10.450 + 0.127(\text{subclass}) + 0.023(\text{subclass})^2 , \quad (2)$$

where the subclass is −1 for M9 V, −0.5 for M9.5 V, 0 for L0 V, 0.5 for L0.5 V, etc. These relations are valid between M9 V and L8 V and are plotted in Figures 8a–8b. With equations (1) and (2) in hand, we can now provide distance estimates to the 62 L dwarfs lacking trigonometric parallaxes in Table 2. Here we compare the measured J and K_s magnitudes with the absolute magnitudes implied by substituting the spectral type into equations (1) and (2). The average of the J and K_s distance estimates is listed in column 11 of Table 2.

Several of these L dwarfs have measured distances or distance estimates that make them eligible for inclusion in the Catalogue of Nearby Stars (Gliese & Jahreiss 1991); i.e., they lie within 25 pc of the Sun. Table 4 lists from Table 2, from Paper I, and from the literature all known L dwarfs that are within or possibly within this 25 pc limit. Also listed are the known T dwarfs believed to be within 25 pc. Table 4 is ordered by spectral type, with the early L dwarfs at the top and T dwarfs at the bottom. This list represents the nearest, brightest examples of each class and as such is the list of choice for further follow-up studies. Columns 1 and 2 list the object name and discovery paper. Columns 3–5 list the spectral type and J and K_s magnitudes. Column 6 lists the estimated distance computed from equation (1), and column 7 lists the estimated distance computed from equation (2).[8] For objects having measured trigonometric parallaxes, columns 6–7 are blank and the measured distance is listed in column 8 instead.

6. THE SPECTROSCOPIC GAP BETWEEN L AND T DWARFS

In Paper I the issue as to whether the L dwarf sequence extends to types later than L8 was also raised. We have calculated that our current search for the latest L dwarfs covers approximately 10% of the sky. Despite this large survey area, however, we still have not identified any L dwarf significantly later than the L8 V presented in Paper I, confirming the conclusions of Paper I. Objects cooler than L8 V *have* been found in the 2MASS data (Burgasser et al. 1999, 2000a), but these are T dwarfs.

Spectroscopically, late L dwarfs and T dwarfs are quite different at J, H, and K bands; T dwarfs have strong bands of CH_4 that are absent in L dwarfs. In the far red, on the other hand, L and T dwarfs are more similar. In this region, the weak FeH bands seen in an L8 V can also be seen in the spectra of some T dwarfs (Burgasser et al. 2000b), and both L and T dwarfs show H_2O, Cs I, and K I absorption (Liebert et al. 2000).

[8] For T dwarfs, distances are estimated using the method of Burgasser et al. (1999).
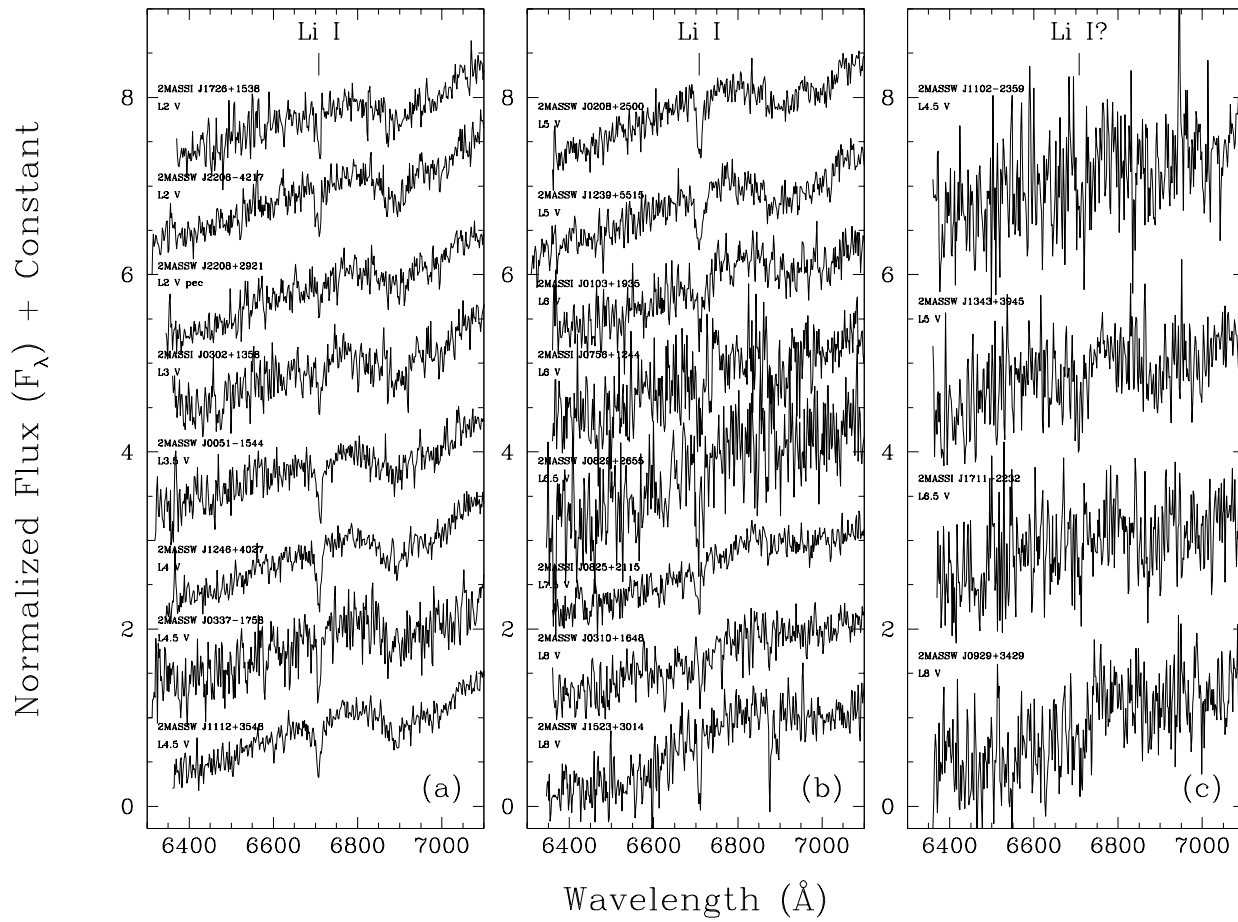
Fig. 6.—(a-b) Detailed spectra of 16 new L dwarfs showing lithium absorption. (a) Detailed spectra of another four new L dwarfs showing possible lithium absorption at our limit of detectability.

The near-infrared spectral differences suggest that objects intermediate between L8 V and the T dwarfs will be difficult to distinguish in the 2MASS data because they presumably would have, at the inception of CH_4 formation, colors intermediate between those of an L8 V $(J-K_s \approx 2.1)$ and a typical T dwarf $(J-K_s \approx 0.0)$. As § 8 below describes more fully, the 2MASS L dwarf discoveries appear to have, within some cosmic scatter, a roughly monotonic relation of $J-K_s$ color with spectral type. That is, there is no evidence that the $J-K_s$ color turns bluer for the L8 V discoveries, yet no L dwarfs with $J-K_s$ colors redder than 2.1 and with types later than L8 have been found, despite exhaustive search efforts.

On the other hand, the spectral similarities in the far red portion of L and T dwarf spectra mean that colors in that region are not affected by the blue reversal seen in the near-infrared. A search of preliminary data from the Sloan Digital Sky Survey (SDSS) has uncovered seven L dwarfs (Fan et al. 2000) and two T dwarfs (Strauss et al. 1999; Tsvetanov et al. 2000) based on $i^* - z^*$ colors, and it appears that the $i^* - z^*$ color may be monotonic across the L-T border. Specifically, $i^* - z^*$ increases from 1.8 at L0 V to 2.3 at L5 V, to 2.6 at L8 V, to ~4 for the two SDSS T dwarfs. (The jump in $i^* - z^*$ color between the latest L dwarfs and the T dwarfs may be caused by the increasing strength of the K I ground-state resonance doublet, which robs the spectrum of much of its i^*-band flux. This may be the analog to the ~1 mag jump in $V-I$ color noted by

Reid et al. [2000] between L4 V and L5 V, an effect thought to be caused by the broadening of the ground-state Na I doublet.) Using SDSS colors, selection for objects intermediate between types L and T would thus be unbiased. Although the statistics are still based on small numbers, no such objects have been identified, despite a successful search for dwarfs on either side of the apparent gap.

These results can be explained if the transition between dwarfs of type L8 V and the known T dwarfs covers a small range in temperature, implying that such intermediate objects are relatively rare. Further observational evidence supports this theory. The best-studied T dwarf, Gl 229B, is known to have a temperature near 950 K (Marley et al. 1996; Allard et al. 1996) and absolute bolometric magnitude of 17.7 (Matthews et al. 1996; Leggett et al. 1999). Based on spectral appearance, the coolest L dwarf known is probably the L8 dwarf 2MASSW J1523226+301456 (Gl 584C). As seen in Table 3, Gl 584C has $M_J = 15.0$, a mere 0.4 mag brighter than the $M_J = 15.4$ value for Gl 229B. Based on the Tinney, Mould, & Reid (1993) measurements of $BC_J = 1.9$ for the M9 dwarf LHS 2924 and $BC_J = 1.7$ for the L4 dwarf GD 165B, we extrapolate to $BC_J \approx 1.3$ for L8 dwarfs such as Gl 584C (see also Reid et al. 1999). This implies $M_{bol} = 16.3$ for Gl 584C. Both Gl 229B and Gl 584C are brown dwarfs and thus to first order have very similar radii (Kumar 1963). Even to second order, because both objects are thought to have masses near $0.045\,M_\odot$ and ages older than ~0.5 Gyr (Kirkpatrick et al. 2000), model calculations
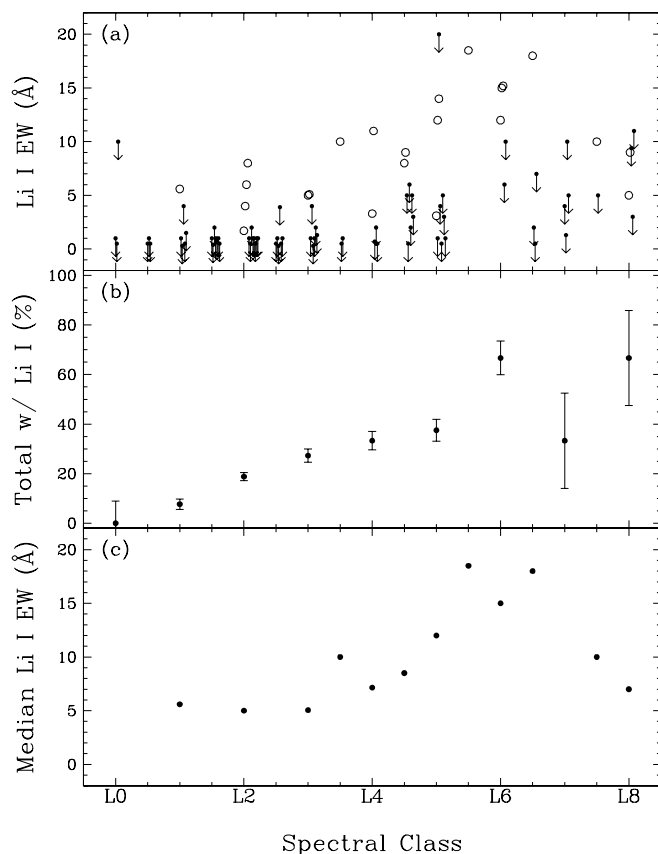
FIG. 7.—(a) Li I equivalent widths as a function of spectral subclass for the 67 L dwarfs from this paper and the 25 L dwarfs from Paper I. Open circles denote objects having a detected Li I absorption line. Downward arrows denote upper limits to the Li I EW for those objects for which no line was detected. To display the data more clearly, some of the points have been given slight offsets along the x-axis. (b) Percentage of L dwarfs showing Li I absorption as a function of spectral subclass. The only objects used in this computation are those for which a Li I equivalent width of 4 Å or more would be detectable. Points have been binned into integer subtypes in which L0 and L0.5 dwarfs have been combined in the L0 bin, L1 and L1.5 dwarfs have been combined in the L1 bin, etc. (c) Median Li strength as a function of spectral class for those objects for which lithium absorption was detected. For spectral subclasses having no objects with detected lithium, no point is plotted. Note the drop in lithium line strength at the latest L types.

FIG. 8.—Absolute magnitude vs. spectral subclass: (a) M_J vs. subclass and (b) M_{K_s} vs. subclass. The second-order fits to each set of data points (given by eqs. [1]–[2]) are also plotted. Absolute magnitudes of two T dwarfs, Gl 229B and Gl 570D, are indicated by the arrows. Note that in (a), the faintest L dwarf (Gl 584C) is only 0.4 mag brighter at J than the T dwarf Gl 229B. In (b), however, this faintest L dwarf is 2.6 mag brighter at K_s than Gl 229B, demonstrating the profound influence that methane has on reshaping the near-infrared spectral energy distribution in the T dwarfs.

show that they should have radii that are very nearly identical (I. Baraffe & G. Chabrier 2000 private communication; Burrows et al. 1997). From the Stefan-Boltzmann law, we can therefore deduce that the temperature difference between Gl 584C and Gl 229B is only ~ 350 K, thus giving Gl 584C $T_{eff} \approx 1300$ K.

Because the available evidence suggests that the T dwarf SDSS 1624+0029 is warmer than Gl 229B (Nakajima et al. 2000; Liebert et al. 2000; Burgasser et al. 2000b), this means that the gap between L8 V and the warmest T dwarfs is less than 350 K. We believe that the temperature range spanned by the gap is *considerably* less than 350 K for two reasons: (1) equilibrium thermochemistry of CO and CH_4 (Lodders 1999; Burrows & Sharp 1999) would suggest that the temperatures of the warmest T dwarfs extend up to 1200 K or above and (2) our confirmation of ~ 100 2MASS discoveries in the ~ 700 K L dwarf temperature range would imply a considerable number of objects falling in a transition region as broad as 350 K, since L dwarfs and 2MASS-observable T dwarfs are known to have similar space

densities. Even though the 2MASS color cuts employed here and by the Burgasser search only partly cover the transition region, the number of objects implied by a 350 K gap would suggest that at least a few of these should have already been detected. All have so far escaped discovery. We conclude, therefore, that the gap must be *much* smaller than 350 K and possibly even less than 100 K.

One final argument in favor of a transition region spanning a very small temperature interval can be made using the recent discovery of the bright T dwarf 2MASSW J0559−1404 (Burgasser et al. 2000c). This object has far weaker methane bands than any other T dwarf, a property that Burgasser et al. ascribe to warmer temperature. This would make 2MASSW J0559−1404 warmer than SDSS 1624+0029, which, as noted above, is believed to be warmer than 950 K. Despite the weaker methane bands in 2MASSW J0559−1404, however, its near-infrared color of $J - K_s = 0.22 \pm 0.06$ is comparable to that of other T dwarfs yet still distinctly bluer, by ~ 1.8 mag, than the average $J - K_s$ value for an L8 V. Forthcoming parallax and bolometric luminosity measurements for 2MASSW J0559−1404 will allow us to determine an accurate temperature, thus allowing better observational constraints on the temperature range spanned by the L-T transition region.

TABLE 3

LATE M, L, AND T DWARFS WITH MEASURED TRIGONOMETRIC PARALLAXES

Dwarf (1)	Type (2)	Ref. for π_{trig} (3)	M_J (mag) (4)	M_{K_s} (mag) (5)
BRI 1222-1222	M9 V	1	11.35 ± 0.15	10.16 ± 0.15
TVLM 868-110639	M9 V	2	11.43 ± 0.08	10.17 ± 0.08
LHS 2065............................	M9 V	3	11.58 ± 0.04	10.30 ± 0.04
LHS 2924............................	M9 V	3	11.78 ± 0.04	10.55 ± 0.04
LP 944-20	M9 V	1	12.24 ± 0.05	11.04 ± 0.05
BRI 0021−0214	M9.5 V	2	11.60 ± 0.09	10.12 ± 0.09
2MASSW J0149090+295613	M9.5 V	4	11.68 ± 0.05	10.26 ± 0.05
2MASP J0345432+254023	L0 V	4	11.88 ± 0.05[a]	10.55 ± 0.06[a]
2MASSI J0746425+200032	L0.5 V	4	11.30 ± 0.04	10.05 ± 0.04
2MASSW J1439284+192915	L1 V	4	11.98 ± 0.04	10.80 ± 0.04
Kelu-1.................................	L2 V	4	11.96 ± 0.09	10.39 ± 0.09
2MASSW J1146345+223053	L3 V	4	12.89 ± 0.08[b]	11.29 ± 0.08[b]
DENIS-P J1058.7−1548	L3 V	4	12.96 ± 0.05	11.31 ± 0.05
2MASSW J0036159+182110	L3.5 V	4	12.74 ± 0.05	11.33 ± 0.04
2MASSW J0326137+295015	L3.5 V	4	12.84 ± 0.12	11.24 ± 0.12
2MASSW J1112257+354813[e]......	L4.5 V	5	12.89 ± 0.06[d]	11.01 ± 0.07[d]
2MASSW J1328550+211449	L5 V	4	13.14 ± 0.42	11.35 ± 0.42
GJ 1001B	L5 V	6	13.20 ± 0.04[d]	11.50 ± 0.04[d]
2MASSW J1507476−162738	L5 V	4	13.41 ± 0.39	11.89 ± 0.39
DENIS-P J1228.2−1547	L5 V	4	13.67 ± 0.13[b]	12.10 ± 0.13[b]
2MASSs J0850359+105716	L6 V	4	14.02 ± 0.36	12.03 ± 0.35
DENIS-P J0205.4−1159	L7 V	4	14.09 ± 0.09[b]	12.53 ± 0.09[b]
2MASSW J1632291+190441	L8 V	4	14.73 ± 0.13	12.85 ± 0.12
2MASSW J1523226+301456[e]......	L8 V	5	14.98 ± 0.12[d]	12.89 ± 0.09[d]
Gl 229B	T dwarf	5	15.4 ± 0.1[d]	15.5 ± 0.1[d]
Gl 570D	T dwarf	5	16.47 ± 0.05[d]	16.41 ± 0.17[d]

NOTE.—For the L and T dwarfs, all spectral types are on the system of Paper I; for the late-M dwarfs, the system of Kirkpatrick, Henry, & Simons (1995). Photometry is taken from 2MASS except for Gl 229B, for which photometry is taken from Matthews et al. (1996). Absolute magnitudes derived from USNO data (Dahn 2000 private communication) use parallaxes updated on 2000 January 4.

[a] Absolute magnitudes are not corrected for the possible duplicity noted in Reid et al. (1999).

[b] Absolute magnitudes have been dimmed by 0.75 mag to account for the fact that this system is a close, equal-magnitude double (Koerner et al. 1999; see also Martín, Brandner, & Basri 1999a for DENIS-P J1228.2−1547.).

[c] Also known as Gl 417B, the widely separated companion to Gl 417A (Kirkpatrick et al. 2000).

[d] The measured parallax for the primary is assumed for the companion.

[e] Also known as Gl 584C, the widely separated companion to Gl 584AB (Kirkpatrick et al. 2000).

REFERENCES.—(1) Tinney 1996; (2) Tinney et al. 1993; (3) Monet et al. 1992; (4) Dahn 2000 private communication; (5) Perryman et al. 1997; (6) van Altena, Lee, & Hoffleit 1995.

7. L DWARF TEMPERATURE SCALE

L0 dwarfs show weaker VO bands than late M dwarfs, presumably because vanadium has begun to condense out of the atmospheres of the L0 dwarfs. Based on the thermo-chemical equilibrium analysis of Lodders (1999), dwarfs of type L0 must then have temperatures near 2000 K, where perovskite formation begins to rob the chromosphere of its vanadium. Thermochemical equilibrium calculations by Burrows & Sharp (1999) also support $T_{eff} \approx 2000$ K for L0 dwarfs. Fits of low-resolution red/near-infrared spectra to atmospheric models including grain and/or dust opacities give $T_{eff} \approx 2000$–2200 K for the M9 dwarf LHS 2924 (Jones & Tsuji 1997; Tsuji, Ohnaka, & Aoki 1996) and $T_{eff} \approx 1900$ K for the L2 dwarf Kelu-1 (Ruiz et al. 1997), again suggest-ing that type L0 has $T_{eff} \approx 2000$ K.

Given the temperature derivation of Gl 584C from the previous section, we can conclude that the L dwarf sequence spans a range of effective temperature from ∼1300 to ∼2000 K. This is in good agreement with the scale sug-gested by Reid et al. (1999) and spans a wider range than the conservative scale proposed in Paper I.

Basri et al. (2000) deduce a temperature range of 1600 to 2200 K for the L dwarf sequence by comparing high-resolution observations of alkali line profiles with Allard's atmospheric models that include dust formation and con-densation. The dusty atmospheres of Tsuji and of Allard, have been used by Pavlenko, Zapatero Osorio, & Rebolo (2000) to show that acceptable fits to the far red spectra of late M, L, and T dwarfs are obtained if an additional opacity source (molecular absorption, dust absorption, or dust scattering) is invoked. These authors derive a tem-perature scale running from 1200 ± 200 K for type L7 V to 2200 ± 200 K for M9.5 V. The intercomparison of results shows that the largest disagreement between scales occurs at the coolest temperatures. Here, more work is needed before model atmospheres produce consistent answers when comparing two different wavelength regimes (such as the far red and the near-infrared) or when comparing high-resolution line profile fits with fits of low-resolution spectral energy distributions. Nevertheless, at this early stage in the study of L dwarfs, it is reassuring that different approaches lead to similar conclusions. Independent determinations of effective temperatures through direct measures of lumi-

TABLE 4

L and T Dwarfs within (or Possibly within) 25 pc of the Sun

Dwarf (1)	Discovery Paper (2)	Type[a] (3)	J (mag)[b] (4)	K_s (mag)[b] (5)	Distance (pc)[c] J (6)	K_s (7)	$\pi_{\rm trig}$ (8)
2MASSI J0746425+200032	Reid et al. 2000	L0.5 V	11.74 ± 0.03	10.49 ± 0.03	...	...	12.3
2MASSW J1412244+163312	This paper	L0.5 V	13.89 ± 0.04	12.59 ± 0.03	25	26	...
2MASSW J1439284+192915	Paper I	L1 V	12.76 ± 0.04	11.58 ± 0.04	...	...	14.3
2MASSW J1300425+191235	Gizis et al. 2000	L1 V	12.71 ± 0.02	11.61 ± 0.03	14	16	...
2MASSW J1108307+683017	Gizis et al. 2000	L1 V	13.14 ± 0.03	11.60 ± 0.03	17	16	...
2MASSW J1658037+702701	Gizis et al. 2000	L1 V	13.31 ± 0.03	11.92 ± 0.03	18	18	...
2MASSW J0208183+254253	This paper	L1 V	14.02 ± 0.03	12.58 ± 0.04	25	25	...
2MASSW J0832045−012835	This paper	L1.5 V	14.13 ± 0.03	12.69 ± 0.03	25	25	...
DENIS-P J1441−0945	Martín et al. 1999b	~L1 V	14.00 ± 0.03	12.64 ± 0.04	25	26	...
Kelu-1	Ruiz et al. 1997	L2 V	13.38 ± 0.03	11.81 ± 0.03	...	...	19.2
2MASSW J0015447+351603	This paper	L2 V	13.82 ± 0.04	12.24 ± 0.03	20	19	...
2MASSW J1338261+414034	This paper	L2.5 V	14.22 ± 0.03	12.75 ± 0.04	23	23	...
2MASSI J1029216+162652	This paper	L2.5 V	14.31 ± 0.04	12.61 ± 0.04	24	22	...
G 196-3B	Rebolo et al. 1998	L2 V	14.90 ± 0.05	12.81 ± 0.13	34	25	...
2MASSW J0036159+182110	Reid et al. 2000	L3.5 V	12.44 ± 0.04	11.03 ± 0.03	...	...	8.7
2MASSW J1506544+132106	Gizis et al. 2000	L3 V	13.41 ± 0.03	11.75 ± 0.03	15	14	...
DENIS-P J1058.7−1548	Delfosse et al. 1997	L3 V	14.18 ± 0.03	12.53 ± 0.03	...	...	17.5
SDSSp J120358.19+001550.3	Fan et al. 2000	~L3 V	14.02 ± 0.03	12.48 ± 0.03	19	19	...
DENIS-P J1047−1815	Martín et al. 1999b	~L3 V	14.20 ± 0.03	12.90 ± 0.03	21	24	...
2MASSW J1615441+355900	This paper	L3 V	14.55 ± 0.04	12.89 ± 0.05	25	23	...
2MASSW J2224438−015852	This paper	L4.5 V	14.05 ± 0.03	12.02 ± 0.03	15	13	...
2MASSW J1112257+354813[d]	This paper	L4.5 V	14.57 ± 0.04	12.69 ± 0.05	...	...	21.7
2MASSW J1246467+402715	This paper	L4 V	15.00 ± 0.04	13.30 ± 0.04	26	25	...
2MASSW J1507476−162738	Reid et al. 2000	L5 V	12.82 ± 0.03	11.30 ± 0.03	...	...	8.:
GJ 1001B	Goldman et al. 1999	L5 V	13.10 ± 0.03	11.40 ± 0.03	...	...	9.6
SDSSp J053951.99−005902.0	Fan et al. 2000	~L5 V	13.99 ± 0.03	12.58 ± 0.03	13	15	...
2MASSW J1239272+551537	This paper	L5 V	14.67 ± 0.03	12.74 ± 0.03	18	16	...
DENIS-P J1228.2−1547AB	Delfosse et al. 1997	L5 V[e]	14.38 ± 0.04[e]	12.81 ± 0.03[e]	...	...	19.6
2MASSW J0205034+125142	This paper	L5 V	15.69 ± 0.06	13.68 ± 0.05	29	25	...
2MASSW J0920122+351742	This paper	L6.5 V	15.59 ± 0.07	13.93 ± 0.08	20	22	...
2MASSI J0825196+211552	This paper	L7.5 V	15.12 ± 0.04	13.05 ± 0.04	13	12	...
DENIS-P J0205.4−1159AB	Delfosse et al. 1997	L7 V[e]	14.55 ± 0.03[e]	12.99 ± 0.04[e]	...	...	17.5
2MASSI J1526140+204341	This paper	L7 V	15.62 ± 0.07	13.92 ± 0.06	18	20	...
2MASSW J1728114+394859	This paper	L7 V	15.96 ± 0.08	13.90 ± 0.05	22	19	...
2MASSW J0030300−145033	This paper	L7 V	16.79 ± 0.16	14.38 ± 0.08	32	24	...
DENIS-P J0255−4700	Martín et al. 1999b	~L8 V	13.23 ± 0.03	11.53 ± 0.03	5	5	...
2MASSW J1632291+190441	Paper I	L8 V	15.86 ± 0.07	13.98 ± 0.05	...	...	16.8
SDSSp J132629.82−003831.5	Fan et al. 2000	~L8 V	16.11 ± 0.07	14.23 ± 0.07	18	18	...
2MASSW J1523226+301456[f]	This paper	L8 V	16.32 ± 0.11	14.24 ± 0.07	...	...	18.6
2MASSW J0310599+164816	This paper	L8 V	16.43 ± 0.11	14.40 ± 0.10	21	20	...
2MASSW J0929336+342952	This paper	L8 V	16.60 ± 0.13	14.62 ± 0.11	23	22	...
2MASSW J0328426+230205	This paper	L8 V	16.67 ± 0.14	14.84 ± 0.13	23	24	...
Gl 229B	Nakajima et al. 1995	T dwarf	14.4 ± 0.1[g]	14.5 ± 0.1[g]	...	...	5.8
Gl 570D	Burgasser et al. 2000a	T dwarf	15.33 ± 0.05	15.27 ± 0.17	...	...	5.9
2MASSW J0559191−140448	Burgasser et al. 2000c	T dwarf	13.83 ± 0.03	13.61 ± 0.05	6	...	...
2MASSW J1225543−273947	Burgasser et al. 1999	T dwarf	15.23 ± 0.05	15.06 ± 0.15	10	...	...
SDSSp J162414.37+002915.6	Strauss et al. 1999	T dwarf	15.53 ± 0.03[h]	15.70 ± 0.05[h]	12	...	...
SDSSp J134646.45−003150.4	Tsvetanov et al. 2000	T dwarf	15.82 ± 0.05[h]	15.84 ± 0.07[h]	13	...	...
2MASSI J1047539+212423	Burgasser et al. 1999	T dwarf	15.82 ± 0.06	>16.29	13	...	...
2MASSW J1217111−031113	Burgasser et al. 1999	T dwarf	15.85 ± 0.07	>15.91	14	...	...
2MASSW J1237392+652615	Burgasser et al. 1999	T dwarf	15.90 ± 0.06	>15.90	14	...	...

[a] All spectral types are on the system of Paper I. Approximate spectral types are given for those objects for which we do not have spectra. For those objects, types have been (re)assigned by eye, based on the published spectra.

[b] Photometry is from 2MASS unless otherwise noted.

[c] Distances are computed from $\pi_{\rm trig}$ when available. For L dwarfs without $\pi_{\rm trig}$ measures, one distance estimate has been computed from the spectral type using equation (1) and the apparent J magnitude, and another has been computed using equation (2) and the apparent K_s magnitude. For T dwarfs without $\pi_{\rm trig}$ measures, the method of Burgasser et al. 1999 has been used to estimate distances from the apparent J magnitude, except for 2MASSW J0559−1404, whose distance estimate comes from Burgasser et al. 2000c.

[d] Also known as Gl 417B. See Kirkpatrick et al. 2000.

[e] This is a combined measure for the AB pair.

[f] Also known as Gl 584C. See Kirkpatrick et al. 2000.

[g] Photometry from Matthews et al. 1996.

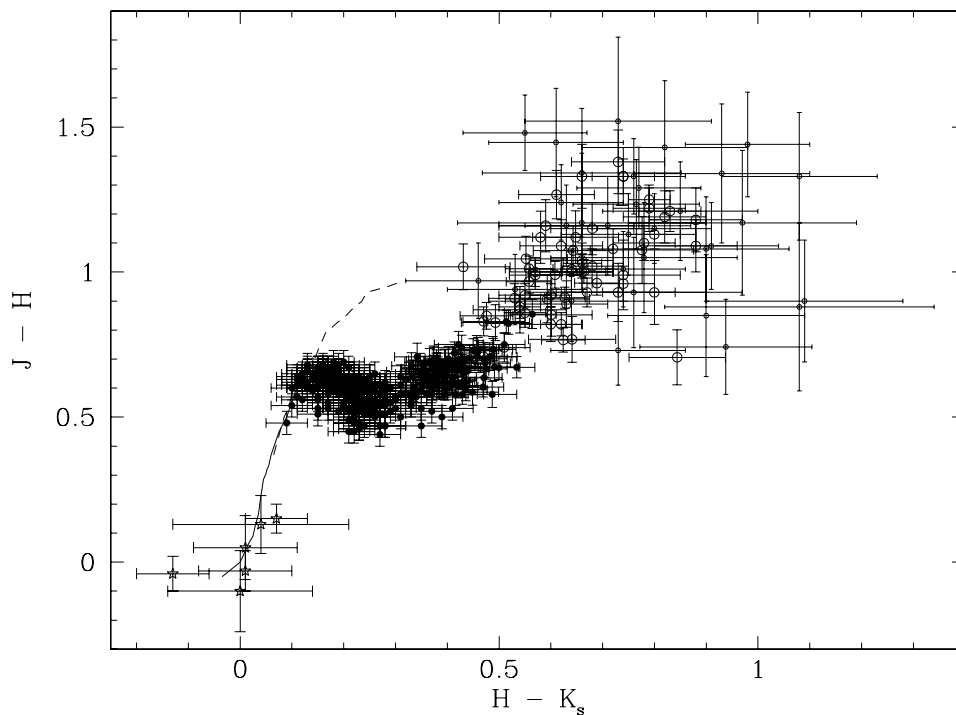[h] Magnitude is from the discovery paper cited. Listed magnitude is K, not K_s.

Fig. 9.—$J-H$ vs. $H-K_s$ for M, L, and T dwarfs. M dwarfs (*filled circles*) are taken from Leggett (1992) and Gizis et al. (2000). L dwarfs (*open circles*) are taken from this paper, Paper I, and Gizis et al. T dwarfs (*stars*) are taken from Matthews et al. (1996), Strauss et al. (1999), Burgasser et al. (1999, 2000a, 2000c), and Tsvetanov et al. (2000). L dwarfs having photometric errors of 0.10 mag or larger in either J, H, or K_s are shown as small open circles, while those with better photometry are shown as large open circles. Tracks for dwarfs (*solid line*) and giants (*dashed line*) from Bessell & Brett (1988) are also plotted. Note that the latest L dwarfs lie at upper right, diagonally opposite their slightly cooler counterparts, the T dwarfs, at lower left.

nosities and radii are, however, still badly needed to constrain and to check the models.

8. COLORS

Armed with a much larger sample of L dwarfs than that presented in Paper I, we can also reinvestigate the color space occupied by L dwarfs and the trends of color with spectral type. Figure 9 shows the $J-H$ versus $H-K_s$ diagram for M dwarfs (*filled circles*), L dwarfs (*open circles*), and T dwarfs (*stars*). Data for the early M dwarfs come from the compilation of Leggett (1992). Colors for late M dwarfs and L dwarfs come from 2MASS data (Gizis et al. 2000; Paper I; this paper). Colors for T dwarfs are taken from 2MASS (Burgasser et al. 1999; 2000a; 2000c) and from the literature (Matthews et al. 1996; Strauss et al. 1999; Tsvetanov et al. 2000). For L dwarfs having 2MASS photometric errors of 0.10 mag or larger in J, H, or K_s, small open circles are plotted; L dwarfs with more accurate magnitudes are plotted as large open circles. Superposed here are the dwarf track (*solid line*; obscured by the M dwarfs in the middle of the diagram) and giant track (*dashed line*) from Bessell & Brett (1988).

This figure shows that L dwarfs lie on a red extension of the familiar dwarf track. Those L dwarfs with well-measured colors (*large open circles*) fall in an area from roughly $(J-H, H-K_s) = (0.8, 0.5)$ to $(1.3, 0.8)$ and have a cosmic scatter similar to that seen for the M dwarfs. However, all indications are that the track abruptly stops at the red end and that slightly cooler objects are sent—via a track on this diagram yet to be observationally determined—to an area near $(J-H, H-K_s) = (0, 0)$ where the T dwarfs lie. Based on arguments in the previous

section, this transition track likely covers a very small range in temperature and thus will contain relatively few objects.

Figure 10 shows the average near-infrared colors of late M through late L dwarfs. Colors have been averaged into spectral class bins with half-subclass spacing. These straight averages (*filled circles*) are plotted as a function of spectral class in Figure 10 and tabulated in Table 5. The number of objects contributing to each average is listed in the last column of Table 5. Also plotted in Figure 10 are the resulting weighted averages (*open circles*), in which objects with more accurately measured photometry are given higher weights than those with poorly measured photometry. These weighted averages should be treated with caution, however, as their resulting errors underestimate the inherent object-to-object scatter in the color measures.

The photometry of Figure 10 and Table 5 is measured by 2MASS and is taken from Gizis et al. (2000), Paper I, and this paper. Colors for types earlier than M8 are not shown because, as Gizis et al. (2000) show, their color-based selection of late M dwarfs is biased at types earlier than this. Two other biases, on the other hand, are still present for this sample of L dwarfs: First, early L types are biased because of the $J-K_s \geq 1.30$ color criterion employed both in Paper I and this paper. This should tend to inflate the observed colors of the early L dwarfs relative to a bias-free sample. This effect is partly mitigated by the inclusion of L dwarfs from Gizis et al. (2000) since a more relaxed color cut was used there, but the number of L dwarfs in their sample is regrettably small. Second, the additional $J-K_s \geq 1.70$ color constraint employed in this paper tends to inflate the colors of mid– to late L dwarfs.

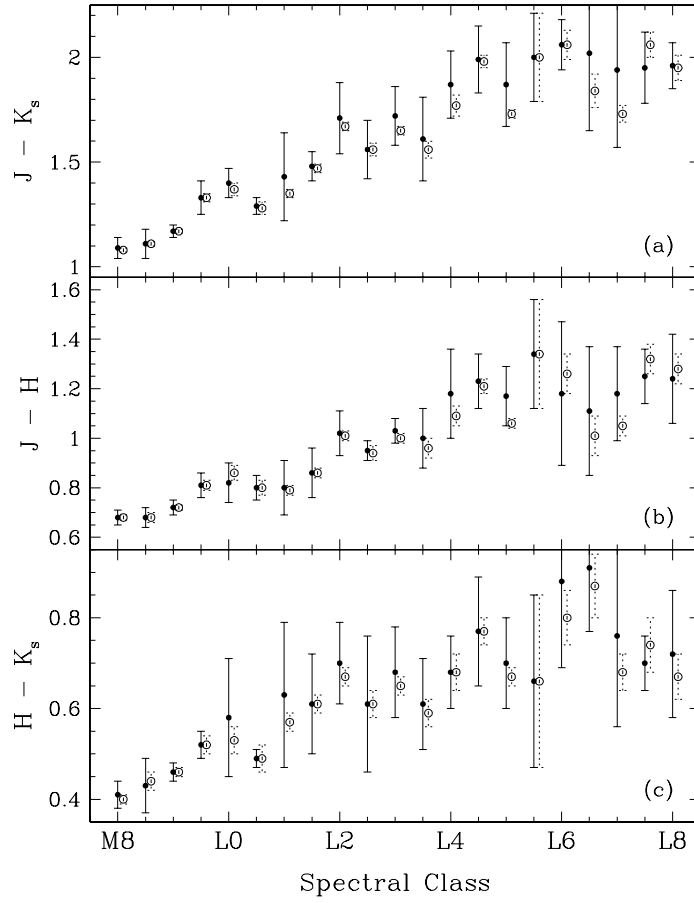Despite these biases, several conclusions can still be made

Fig. 10.—Near-infrared color vs. spectral class for late M through late L dwarfs: (a) $J-K_s$, (b) $J-H$, and (c) $H-K_s$. Filled circles are plotted for the averages listed in Table 5. Open circles are weighted averages that give a higher weight to colors with smaller measurement errors. See text for details. All data shown here are from 2MASS and are taken from this paper, Paper I, and Gizis et al. (2000).

TABLE 5
AVERAGE NEAR-INFRARED COLORS FOR LATE M AND L DWARFS[a]

Sp. Type (1)	$\langle J-K_s \rangle$ (2)	$\sigma_{\langle J-K_s \rangle}$ (3)	$\langle J-H \rangle$ (4)	$\sigma_{\langle J-H \rangle}$ (5)	$\langle H-K_s \rangle$ (6)	$\sigma_{\langle H-K_s \rangle}$ (7)	No. used in Ave. (8)
M8........	1.09	0.05	0.68	0.03	0.41	0.03	14
M8.5......	1.11	0.07	0.68	0.04	0.43	0.06	7
M9........	1.17	0.03	0.72	0.03	0.46	0.02	9
M9.5......	1.33	0.08	0.81	0.05	0.52	0.03	4
L0	1.40	0.07	0.82	0.08	0.58	0.13	3
L0.5	1.29	0.04	0.80	0.05	0.49	0.02	3
L1	1.43	0.21	0.80	0.11	0.63	0.16	8
L1.5	1.48	0.07	0.86	0.10	0.61	0.11	8
L2	1.71	0.17	1.02	0.09	0.70	0.09	12
L2.5	1.56	0.14	0.95	0.04	0.61	0.15	5
L3	1.72	0.14	1.03	0.05	0.68	0.10	9
L3.5	1.61	0.20	1.00	0.12	0.61	0.10	3
L4	1.87	0.16	1.18	0.18	0.68	0.08	4
L4.5	1.99	0.16	1.23	0.11	0.77	0.12	8
L5	1.87	0.20	1.17	0.12	0.70	0.10	10
L5.5	2.00	0.21	1.34	0.22	0.66	0.19	1
L6	2.06	0.12	1.18	0.29	0.88	0.19	5
L6.5	2.02	0.37	1.11	0.26	0.91	0.14	4
L7	1.94	0.37	1.18	0.19	0.76	0.20	4
L7.5	1.95	0.17	1.25	0.11	0.70	0.06	2
L8	1.96	0.11	1.24	0.18	0.72	0.14	5

[a] All photometry is from 2MASS.

based on Figure 10:

1. Within the scatter of the points, $J - K_s$ color increases monotonically from late M through late L spectral types and has a maximum of $J - K_s \approx 2.1$ for the late L dwarfs. Even though the $J - K_s$ color appears to level off near 2.0 at types of $\sim$L5 and later, the $J - K_s \geq 1.70$ bias discussed above may have artifically inflated the colors of the mid–L dwarfs relative to the late L dwarfs. The structure seen at early L types may also be an artifact of the $J - K_s \geq 1.30$ bias having inflated the colors of L0 and L1 dwarfs and the L0.5 bin having been based on only three objects.

2. Given the same arguments above, it also appears that the $J - H$ color increases roughly monotonically with spectral type for L dwarfs.

3. $H - K_s$ color also appears to increase roughly monotonically with increasing spectral type, at least through mid–L. At late L types, though, the $H - K_s$ color may turn slightly bluer. The $H - K_s$ color, however, covers a smaller range than the other two colors, and the dispersions are also quite large. If there is a blueward dip at the latest L types, it may mean that the pressure-induced H_2 opacity has increased markedly at the K_s band. Tokunaga & Kobayashi (1999) overplot the L2 dwarf Kelu-1 with the L4 dwarf GD 165B and the L7 dwarf DENIS-P J0205.4−1159AB and show that the late L object has a flux deficit at the K band relative to the other two L dwarfs, a deficit which they ascribe to increased collision-induced absorption by molecular hydrogen. This possible blueward dip of $H - K_s$ color for the late L dwarfs and (if verified) its cause need to be studied further with improved photometry and near-infrared spectroscopic follow-up.

Figure 8 has shown that absolute J and K_s magnitudes are well correlated with L dwarf spectral subclass. As shown in Figure 11, however, the correlation of M_J and M_{K_s} with

individual $J - K_s$ colors exhibits much larger scatter than the correlation of M_J and M_{K_s} with spectral type. In other words, L dwarf distance estimates derived from $J - K_s$ colors have much larger uncertainties than those derived from spectral type. Part of this scatter is simply due to the uncertainties in 2MASS photometry, typically ± 0.07 mag for $J - K_s$ though occasionally larger. More importantly, perhaps, this figure demonstrates the intrinsic limitation of estimating spectral types and photometric distances using colors of small baseline. An additional, possible reason for the larger scatter in Figures 11b and 11d is that our spectral type is derived from far red spectra, and here dust may be playing a minimal role in shaping the spectrum. In the near-infrared, on the other hand, the presence of dust can lead to a backwarming of the atmosphere, and this will alter the amount of H_2O and H_2 in the photosphere. Because both of these molecules play a critical role in shaping the near-infrared spectrum, slight object-to-object variations in their opacities can lead to differences in near-infrared colors (Chabrier et al. 2000).

9. CONCLUSIONS

We present spectra for another 67 L dwarfs discovered during follow-up of sources identified by 2MASS. These, together with L dwarfs from Paper I, from Gizis et al. (2000), and from other surveys such as SDSS and DENIS, bring the total of known L dwarfs to well over 100. This sample can be used for a variety of follow-up investigations. The presence of Hα emission is seen to decline rapidly from early to mid–L dwarfs, and Hα emission is not seen in any L dwarf later than type L4.5. If the lack of Hα emission is an indicator of youth and/or substellarity as Gizis et al. (2000) suggest, then the ratio of Hα-emitters to nonemitters at any given L subtype may reflect the ratio of stars to brown dwarfs at that class. Lithium absorption, when detected, is
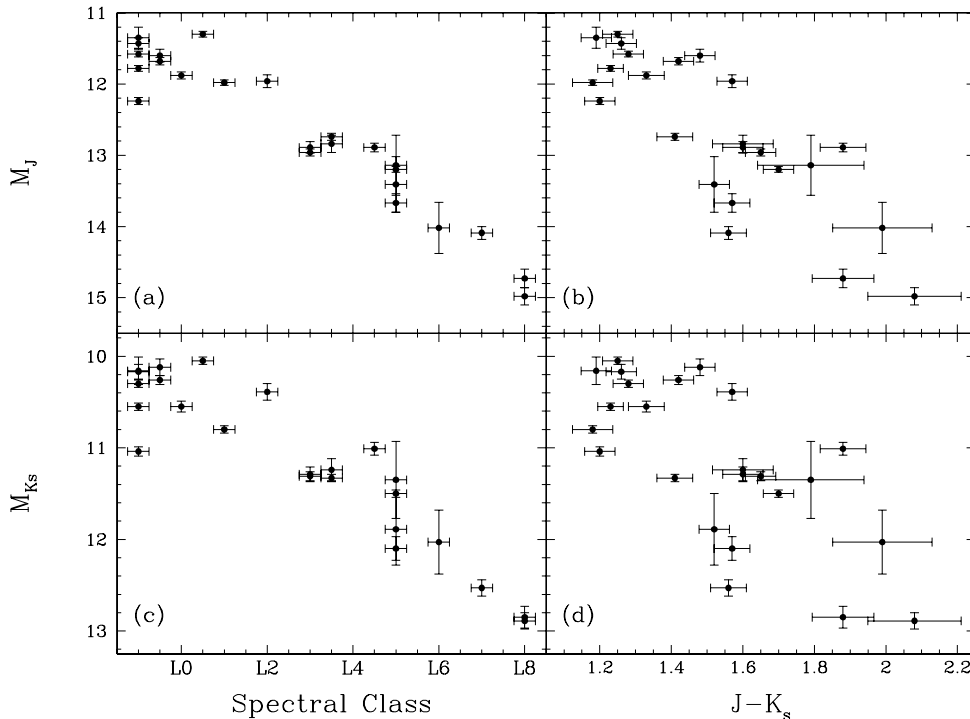

FIG. 11.—Comparison of absolute magnitude vs. spectral type to absolute magnitude vs. $J - K_s$ color for dwarfs of type M9 through L8. (a–b) M_J and (c–d) M_{K_s}. Panels (a) and (c) are taken from Fig. 8. Note the markedly increased scatter in the color relation compared with the spectral type relation. See text for details.

seen to increase in strength from early to mid–L types, but then declines markedly after type L6.5 V. This turnover in lithium strength may herald the depletion of atomic lithium into lithium-bearing molecules and as such would provide a vital clue to the temperature scale for L dwarfs because these reactions are expected roughly around 1500 K. The difference in temperature between the latest L dwarf and Gl 229B is calculated at ~ 350 K. This means that the gap in temperature between L8 and the warmest of the known T dwarfs must be significantly less that 350 K, as several of the known T dwarfs are suspected of being warmer than Gl 229B itself. This also means that L dwarfs span the likely temperature range 1300 K $\lesssim T_{\rm eff} \lesssim$ 2000 K. The locus of L dwarfs in near-infrared color space is also shown, and distance estimates are made for all L and T dwarfs lacking trigonometric parallax measurements. Even at this early stage in our investigations, researchers have identified 53 L and T dwarfs known (or suspected) to be within 25 pc of the Sun, clearly indicating that this previously hidden population of cool objects is very large.

REFERENCES

Allard, F., Hauschildt, P. H., Baraffe, I., & Chabrier, G. 1996, ApJ, 465, L123
Basri, G., Mohanty, S., Allard, F., Hauschildt, P. H., Delfosse, X., Martín, E. L., Forveille, T., & Goldman, B. 2000, ApJ, in press
Becklin, E. E., & Zuckerman, B. 1988, Nature, 336, 656
Bessell, M. S., & Brett, J. M. 1988, PASP, 100, 1134
Burgasser, A. J., et al. 1999, ApJ, 522, L65
———. 2000a, ApJ, 531, L57
Burgasser, A. J., Kirkpatrick, J. D., Reid, I. N., Liebert, J., Gizis, J. E. & Brown, M. E. 2000b, AJ, in press
Burgasser, A. J., et al. 2000c, AJ, in press
Burrows, A., et al. 1997, ApJ, 491, 856
Burrows, A., & Sharp, C. M. 1999, ApJ, 512, 843
Chabrier, G., Baraffe, I., Allard, F., & Hauschildt, P. 2000, ApJ, in press
Cuby, J. G., Saracco, P., Moorwood, A. F. M., D'Odorico, S., Lidman, C., Comerón, F., & Spyromilio, J. 1999, A&A, 349, L41
Delfosse, X., et al. 1997, A&A, 327, L25
Fan, X., et al. 2000, AJ, 119, 928
Gizis, J. E., Monet, D. G., Reid, I. N., Kirkpatrick, J. D., Liebert, J., & Williams, R. J. 2000, AJ, in press
Gliese, W., & Jahreiss, H. 1991, CD ROM, Preliminary Version of the Third Catalogue of Nearby Stars, Vol. 1, No. 1 (NSSDC/ADC) (Greenbelt, MD: GSFC)
Goldman, B. et al. 1999, A&A, 351, L5
Hamuy, M., Suntzeff, N. B., Heathcote, S. R., Walker, A. R., Gigoux, P., & Phillips, M. M. 1994, PASP, 106, 566
Jones, H. R. A., & Tsuji, T. 1997, ApJ, 480, L39
Kirkpatrick, J. D., Burgasser, A. J., Gizis, J. E., Reid, I. N., Dahn, C. C., & Monet, D. G. 2000, in preparation
Kirkpatrick, J. D., Henry, T. J., & Liebert, J. 1993, ApJ, 406, 701
Kirkpatrick, J. D., Henry, T. J., & Simons, D. A. 1995, AJ, 109, 797
Kirkpatrick, J. D., et al. 1999, ApJ, 519, 802 (Paper I)

Koerner, D. W., Kirkpatrick, J. D., McElwain, M. W., & Bonaventura, N. R. 1999, ApJ, 526, L25
Kumar, S. S. 1963, ApJ, 137, L1121
Leggett, S. K. 1992, ApJS, 82, 351
Leggett, S. K., Toomey, D. W., Geballe, T. R., & Brown, R. H. 1999, ApJ, 517, L139
Liebert, J., Reid, I. N., Burrows, A., Burgasser, A. J., Kirkpatrick J. D., & Gizis, J. E. 2000, ApJ, 533, L155
Lodders, K. 1999, ApJ, 519, 793
Marley, M. S., Saumon, D., Guillot, T., Freedman, R. S., Hubbard, W. B., Burrows, A., & Lunine, J. I. 1996, Science, 272, 1919
Martín, E. L., Brandner, W., & Basri, G. 1999a, Science, 283, 1718
Martín, E., Delfosse, X., Basri, G., Goldman, B., Forveille, T., & Zapatero Osorio, M. R. 1999b, AJ, 118, 2466
Matthews, K., Nakajima, T., Kulkarni, S. R., & Oppenheimer, B. R. 1996, AJ, 112, 1678
Monet, D. G., Dahn, C. C., Vrba, F. J., Harris, H. C., Pier, J. R., Luginbuhl, C. B., & Ables, H. D. 1992, AJ, 103, 638
Nakajima, T., Oppenheimer, B. R., Kulkarni, S. R., Golimowski, D. A., Matthews, K., & Durrance, S. T. 1995, Nature, 378, 463
Nakajima, T., et al. 2000, PASJ, 52, 87
Oke, J. B., et al. 1995, PASP, 107, 375
Oke, J. B., & Gunn, J. E. 1982, PASP, 94, 586
Oppenheimer, B. R., Kulkarni, S. R., Matthews, K., & Nakajima, T. 1995, Science, 270, 1478
Pavlenko, Y., Zapatero Osorio, M. R., & Rebolo, R. 2000, A&A, 355, 245
Perryman, M. A. C., et al. 1997, A&A, 323, L49
Rebolo, R., Zapatero Osorio, M. R., Madruga, S., Béjar, V. J. S., Arribas, S., & Licandro, J. 1998, Science, 282, 1309
Reid, I. N., Kirkpatrick, J. D., Gizis, J. E., Dahn, C. C., Monet, D. G., Williams, R. J., Liebert, J., & Burgasser, A. J. 2000, AJ, 119, 369
Reid, I. N., et al. 1999, ApJ, 521, 613

Ruiz, M. T., Leggett, S. K., & Allard, F. 1997, ApJ, 491, L107
Strauss, M. A., et al. 1999, ApJ, 522, L61
Tinney, C. G. 1996, MNRAS, 281, 644
Tinney, C. G., Mould, J. R., & Reid, I. N. 1993, AJ, 105, 1045
Tokunaga, A. T., & Kobayashi, N. 1999, AJ, 117, 1010

Tsuji, T., Ohnaka, K., & Aoki, W. 1996, A&A, 305, L1
Tsvetanov, Z., et al. 2000, ApJ, 531, L61
van Altena, W. F., Lee, J. T., & Hoffleit, E. D. 1995, The General Catalogue
    of Trigonometric Stellar Parallaxes (4th ed.; Schenectady: L. Davis)

Note added in proof.—After submission of this paper, SDSS (Leggett et al. 2000, ApJL, in press) announced the discovery of three early T dwarfs in the spectroscopic gap between late L dwarfs and previously known T dwarfs.